Chemical Reviews

NORMAL MODES AND GROUP FREQUENCIES—CONFLICT OR COMPROMISE? AN IN-DEPTH VIBRATIONAL ANALYSIS OF CYCLOHEXANONE†

H. FUHRER,‡ V. B. KARTHA,‡ P. J. KRUEGER,# H. H. MANTSCH,‡ AND R. N. JONES*

Division of Chemistry, National Research Council of Canada, Ottawa, Canada

Contents

I. Introduction

Organic chemists interpret infrared and Raman spectra in terms of characteristic group frequencies. Attention centers on bands known to be associated with specific molecular structure, and the rest of the spectrum is disregarded save for purposes of empirical fingerprint identification. Group frequency analysis has proved valuable in the determination of structure, and interest reached a zenith in the 1950's when several monographs appeared. These still provide an adequate account; more recent articles deal mainly with applications to specific types of compounds and with rationalizations of small band displacements in terms of steric, inductive, and electronic field effects. The decline in the discovery of new group frequencies has been noted by Bellamy.[1]

Molecular spectroscopists prefer to treat the molecule as a dynamic whole and classify vibratory motion by normal coordinate analysis. This requires that both the infrared and

Raman spectra be known completely, including the polarization of the Raman bands; a knowledge of the contours of the infrared bands measured in the gas phase is also helpful. Until recently normal coordinate analysis has been applied only to small symmetric molecules, to hydrocarbons, and to syntactic polymers with high symmetry in the repeating unit. The analysis rapidly becomes more difficult as the molecule gets larger and the symmetry diminishes.

A complete normal coordinate analysis yields a quantitative description of the vibrational motions of all the atoms in terms of a set of force constants defining the resistance of each bond to stretch and torsion, and of all inter-bond angles to deformation. Such force fields must be interpreted cautiously since more than one set of force constants can yield calculated vibrational frequencies in agreement with those observed experimentally. This has led some spectroscopists to warn against the uncritical use of force constant calculations,[2,3] and the pitfalls have been demonstrated by Long, Gravenor, and Woodger.[4] Although this ambiguity is ever present, its significance diminishes when a set of isotopically substituted molecules is analyzed concurrently, and the reliance to be placed on the calculations augments with the number of isotopic species involved.

Some chemical spectroscopists attempt to interpret the vibrational spectra of more complex molecules by a transposition of the results of normal coordinate analysis of simpler molecules, often aided by qualitative comparisons of the spectra of isotopically substituted species, and the polarizations of the Raman bands. It has become an accepted practice to include tables of these "vibrational assignments" in publications on the infrared and Raman spectra of larger molecules. It is difficult to resist the challenge this presents to make such "assignments" for all the bands in the spectra, but while some of the assignments may be credible, others can be highly speculative. Furthermore the modes assigned to these vibrations are often grossly oversimplified in an attempt to describe them as group frequencies in localized bond systems.

Most organic molecules are too large and asymmetric for even such qualitative attempts at a detailed description of their vibrational spectra. This is well illustrated by steroids,

---

(1) L. J. Bellamy, Preface to "Advances in Infrared Group Frequencies", Methuen, London, 1968.

---

(2) P. J. Hendra, *Annu. Rep. Progr. Chem.*, **64A**, 199 (1967).
(3) D. A. Long, *ibid.*, **65A**, 105 (1968).
(4) D. A. Long, R. B. Gravenor, and M. Woodger, *Spectrochim. Acta*, **19**, 937 (1963).

whose infrared spectra have been documented extensively for purposes of empirical identification, and several hundred are now on file. Below 1300 cm^{-1} few of the bands in these spectra can be correlated with specific molecular structure; where this is possible the bands are assigned to the C–O stretch and to O–H bend motions in functional groups and to deformations of aromatic and olefinic C–H bonds. In spite of the failure to identify many group frequencies, comparisons among the infrared spectra of steroids do permit sets of bands extending through the fingerprint region (1500–600 cm^{-1}) to be identified with stereospecific elements of the molecular structure. These have been tabulated for hydroxy steroids,[5] keto steroids,[6] acetoxy steroids,[7] and steroidal sapogenins.[8] They can also be recognized as superimposed sets of bands in steroids containing more than one functional group.[9]

Evidence that the fingerprint regions of the infrared spectra of complex molecules contain as yet uncorrelated sets of structurally significant bands, transferable among compounds of the same chemical family, has come recently from another direction. In our laboratory we have been searching the ASTM computer-based catalog of some 100,000 infrared spectra[10] by a pattern recognition program FIRST-1 developed by Erley.[11] This has demonstrated that the computer identification of organic compounds from their infrared spectra is highly effective, even when the search is made solely on the spectral pattern without benefit of additional chemical criteria. The substances searched for have included polynuclear aromatic hydrocarbons, heterocyclic compounds containing nitrogen or sulfur, and simple open and caged alicyclic compounds as well as steroids. The program extracts from the master file the 20 spectra that most closely match the submitted pattern data; it lists them in a sequence of diminishing closeness of fit on a figure-of-merit scale from 100 to 0. Almost invariably the compounds having a figure of merit above 70 are found to belong to the same chemical family as the test substance. This is clearly indicative of common spectral features in the fingerprint spectra that await more specific identification. Most of the peaks used in these search routines are not the well-characterized group frequency bands.

Digital computers make it feasible to extend the methods of normal coodinate analysis to larger and less symmetric molecules, and typical examples of low symmetry structures studied by this means are cyclohexene,[12] *trans*-decalin,[13] and poly-L-alanine.[14] The problems have been discussed in general terms by Califano[15] and with specific reference to polymers by Zerbi.[16]

If an attempt is made to use the general valence force field,

which takes account of all interatomic forces, the computation is impossibly complex. However, this can be circumvented by a judicious use of chemical intuition to include only those near-neighbor interatomic forces that can reasonably be expected to have chemical significance. A carefully chosen *selective valence force field*[17] that will permit the semiquantitative interpretation of all the main features of the infrared and Raman spectra of complex molecules could help to resolve the long-standing dichotomy between the physical and the organic chemist in the analysis of molecular vibration spectra.

These considerations led us to undertake normal coordinate calculations on molecules somewhat more complex than those generally studied in the past; the molecules selected offer potential stepping stones to terpenes, steroids, and other compounds of biological interest. As a starting point to gain familiarity with the computational techniques, the spectra of the trans–trans conformer of diethyl ether were analyzed, and the optimized force field was used to compute the spectra of the less symmetric trans–gauche conformer with which it is in equilibrium at room temperature.[18] In this review the establishment of an acceptable force field for cyclohexanone is described in depth; this provides an excellent basis for the discussion of many general problems that arise in the course of such calculations and which are commonly glossed over. More technical details of the numerical aspects of the computations, including listings of the relevant computer programs, will be published separately.[19]

The possibility of establishing sets of force constants transferable from one molecule to another is attractive, but much of the skepticism about the value of force constant calculations centers on this concept.[2,4] Discussion of this will be deferred to a later publication dealing with cyclopentanone,[20] but it should be noted here that other types of selective force fields can be used. Shimanouchi and collaborators[21,22] have made extensive studies of the transferability of force fields of the Urey–Bradley type[23] and demonstrated their efficacy for a wide range of molecular structures. We have carried out parallel series of computations on cyclohexanone using Urey–Bradley force fields, but we prefer to put the emphasis on the selective valence force field method, because the picture of the vibrating molecule which it generates conforms more closely with the chemist's visualization of the molecular dynamics. The Urey–Bradley fields stress the forces between nonbonded atoms. Although field effects of this kind undoubtedly play a part in stabilizing molecular structures, they are not yet well understood; both repulsive and attractive factors must be taken into account, and these are difficult to assess.[24] In the present state of our knowledge, a dynamic model based solely on the forces acting through the bond system seems more

(5) R. N. Jones, F. Herling, and E. Katzenellenbogen, *J. Amer. Chem. Soc.*, **77**, 651 (1955).

(6) R. N. Jones and G. Roberts, *ibid.*, **80**, 6121 (1958).

(7) R. N. Jones and F. Herling, *ibid.*, **78**, 1152 (1956).

(8) R. N. Jones, E. Katzenellenbogen, and K. Dobriner, *ibid.*, **75**, 158 (1953).

(9) R. N. Jones, *Trans. Roy. Soc. Can.*, *Sect. 3*, **52**, 9 (1958).

(10) ASTM Serial Number List of Compound Names and References to Published Infrared Spectra, No. AMD-32, American Society for Testing and Materials, Philadelphia, Pa., 1969.

(11) This is an updated version of the program SIRCH-1 described by D. S. Erley, *Anal. Chem.*, **40**, 894 (1968); *Appl. Spectrosc.*, **25**, 200 (1971).

(12) N. Neto, C. Di Lauro, E. Castellucci, and S. Califano, *Spectrochim. Acta, Part A*, **23**, 1763 (1967).

(13) R. G. Snyder and J. H. Schachtschneider, *Spectrochim. Acta*, **21**, 169 (1965).

(14) K. Itoh and T Shimanouchi, *Biopolymers*, **9**, 383 (1970).

(15) S. Califano, *Pure Appl. Chem.*, **18**, 353 (1969).

(16) G. Zerbi, *Appl. Spectrosc. Rev.*, **2**, 193 (1969).

(17) This is also referred to in the literature as a *modified valence force field*.

(18) H. Wieser, W. G. Laidlaw, P. J. Krueger, and H. Fuhrer, *Spectrochim. Acta, Part A*, **24**, 1055 (1968).

(19) H. Fuhrer, V. B. Kartha, G. Kidd, P. J. Krueger, H. H. Mantsch, and R. N. Jones, *Nat. Res. Counc. Can.*, *NCR Bull.*, in preparation.

(20) V. B. Kartha, H. H. Mantsch, and R. N. Jones, in preparation.

(21) T. Shimanouchi, *J. Chem. Phys.*, **17**, 245, 848 (1949); International Symposium on Molecular Structure and Spectroscopy C-216, Tokyo, 1962.

(22) T. Shimanouchi in "Physical Chemistry, An Advanced Treatise," Vol. IV, H. Eyring, D. Henderson, and W. Jost, Eds., Academic Press, New York, N. Y., 1970, Chapter 6.

(23) H. C. Urey and C. A. Bradley, *Phys. Rev.*, **38**, 1969 (1931).

(24) See pp 295–297 of ref 22 and the other references cited therein.

readily interpretable in chemical terms, particularly for complex molecules of low symmetry.

II. Setting up the Vibrational Computation

Initiating a normal coordinate calculation is basically the same whether the structure be simple or complex; the matrix algebra is not affected and only the matrices themselves become more elaborate as the molecule becomes larger. Detailed descriptions of the theory are available in several monographs, notably those of Wilson, Decius, and Cross[25] and Shimanouchi;[22] a succinct account has been given by Mills.[26]

It is unfortunate that the sophistication of the mathematics has restricted interest in normal coordinate calculations to a coterie of molecular spectroscopists. It is probable that the chemist rather than the physicist has more to gain from vibrational studies on large molecules, and we shall describe the setting up of the vibrational computations for cyclohexanone with more emphasis on the chemical aspects than is to be found in the standard texts.

A. MOLECULAR GEOMETRY AND INTERNAL COORDINATE SYSTEM OF CYCLOHEXANONE

The geometry of cyclohexanone in the energetically favored chair conformation has been described by Tai and Allinger.[27] The optimal bond lengths and valence angles are shown in Figure 1 where the atoms are numbered arbitrarily from 1 to 17 starting with oxygen. From these structural parameters the *Cartesian coordinates* of the equilibrium positions of the atoms can be listed in a matrix X. The determination of the Cartesian coordinates for all the atoms in a large molecule may be a time-consuming and laborious task, particularly if the symmetry is low. The approach to be followed to simplify this step will depend on the structural parameters for the molecule which are available (or which are assumed). Invariably these consist of interatomic distances and interbond angles. If the torsional angles about all bonds are known (or can be assumed), the computer program CART will conveniently provide the Cartesian coordinates.[19] In other cases basic trigonometric relations of three-dimensional geometry may have to be used to determine the torsional angles, or the Cartesian coordinates themselves. In the case of cyclohexanone the oxygen atom is chosen as the origin of coordinates, and the values in Table I are taken from the data of Tai and Allinger.[28]

Normal coordinate calculations are now almost universally based on the F and G matrix method of Wilson, Decius, and Cross.[25] The G matrix lists the kinetic properties of the system and separates the vibrational from the translational and rotational energies. It requires that the vibrational displacements be expressed as changes in bond lengths (r, d, v), bond angles (γ, δ, ω, χ, ϵ), out-of-plane bends (ρ), and torsions (τ).

Figure 1. Structural parameters of cyclohexanone in the chair conformation.

Table I

Cartesian Coordinates for Cyclohexanone (Chair)[a]

Atom no.	Coordinates, Å		Atom no.	Coordinates, Å	
1 (O)	x	0.0	10 (H_{ax})	x	2.60859
	y	0.0		y	-1.33512
	z	0.0		z	2.07753
2 (C)	x	1.22	11 (H_{eq})	x	3.73177
	y	0.0		y	-2.15034
	z	0.0		z	0.97651
3 (C)	x	2.01488	12 (H_{ax})	x	2.49096
	y	1.27208		y	-1.40687
	z	0.0		z	-0.98245
4 (C)	x	3.08838	13 (H_{eq})	x	1.33959
	y	1.26543		y	-2.12632
	z	1.09017		z	0.15568
5 (C)	x	3.94614	14 (H_{ax})	x	2.49096
	y	0.0		y	1.40687
	z	1.02825		z	-0.98245
6 (C)	x	3.08838	15 (H_{eq})	x	1.33959
	y	-1.26543		y	2.12632
	z	1.09017		z	0.15568
7 (C)	x	2.01488	16 (H_{ax})	x	2.60859
	y	-1.27208		y	1.33512
	z	0.0		z	2.07753
8 (H_{eq})	x	4.66041	17 (H_{eq})	x	3.73177
	y	0.0		y	2.15034
	z	1.86480		z	0.97651
9 (H_{ax})	x	4.53286			
	y	0.0			
	z	0.09778			

[a] For numbering of atoms see Figure 1.

These are the *internal valence coordinates* listed in a matrix B. They are illustrated in Figure 2; there are 57 in all and in Figure 3 they are numerically identified. Once this set of valence coordinates has been defined, the relation with the Cartesian coordinate system can be established by means of a computer program GMAT[19] which performs the multiplication

$$R = BX \qquad (1)$$

(25) E. B. Wilson, Jr., J. C. Decius, and P. C. Cross, "Molecular Vibrations. The Theory of Infrared and Raman Vibrational Spectra," McGraw-Hill, New York, N. Y., 1955.

(26) I. M. Mills in "Infra-red Spectroscopy and Molecular Structure," M. Davies, Ed., Elsevier, Amsterdam, 1963, pp 166-198.

(27) J. C. Tai and N. L. Allinger, *J. Amer. Chem. Soc.*, **88**, 2179 (1966).

(28) The conventions used by Tai and Allinger to define the equatorial and axial bonds differ from those of most organic chemists. In their system the C–H bond having the smaller absolute value of the z coordinate is always equatorial. This causes their "equatorial" and "axial" bonds at C₄ (atom 5 of Figure 1) to be transposed from the conventional assignments for the chair conformation of cyclohexane. This has been changed in our Table I which follows conventional practice; our axial C–H at C₄ is approximately perpendicular to the plane defined by C₂, C₄, and C₆ (atoms 3, 5, 7 of Figure 1) as it is in cyclohexane.
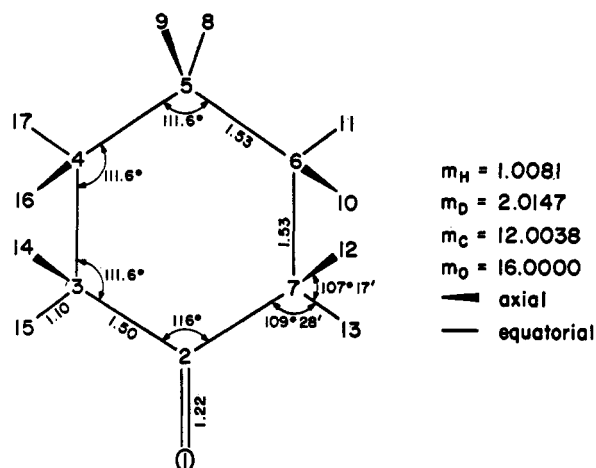
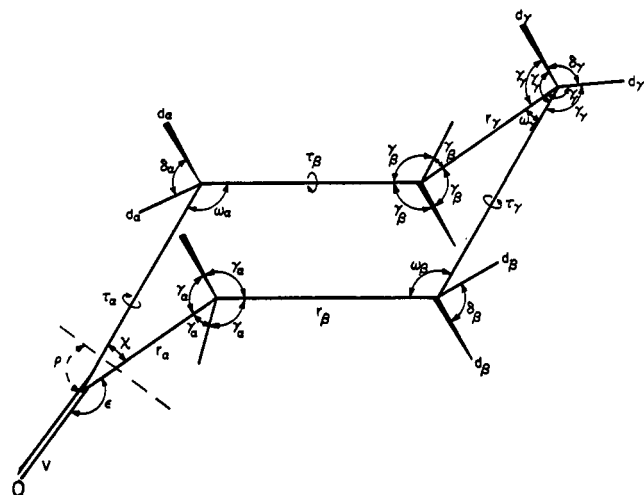**Figure 2.** Internal valence coordinates

Figure 3. Numerical identification of internal valence coordinates

to generate a transformation matrix **B**. The same program will also generate the **G** matrix if the masses of the atoms are supplied (Figure 1) where

$$G = BM^{-1}B' \quad (2)$$

and M^{-1} is a matrix of the reciprocal masses.[29]

The kinetic energy (T) is given by the expression

$$2T = \dot{R}'G^{-1}\dot{R} \quad (3)$$

where $\dot{R}_i$ is the time derivative ($\delta R_i/\delta t$) of the ith valence coordinate.

B. TRANSPOSITION TO SYMMETRY COORDINATES

The geometry assumed for cyclohexanone possesses a single element of symmetry, a plane through atoms 1, 2, 5, 8, 9. This yields two species of vibrations A' and A'' which are respectively symmetric and antisymmetric to the symmetry plane. This system belongs to the point group C_s, and the 17 atoms are associated with 45 nondegenerate normal vibrations.[30] Of these, 25 belong to the A' species and 20 to the A'' species.[31]

Because the number of internal coordinates (57) exceeds the number of normal coordinates of nonzero frequency (45),[32] the internal coordinates can be converted to *symmetry coordinates* using a transformation matrix **U**.

$$S = UR \quad (4)$$

The choice of these nonnormalized symmetry coordinates is shown in Table II. It is in the setting up of this coordinate system that the first element of chemical intuition is injected

into the calculations, and it will be apparent that these symmetry coordinates have been selected to conform closely with group frequencies.

In addition to their intrinsic chemical appeal, symmetry coordinates have several computational advantages. In the first place they permit use to be made of the symmetry, since they can be factored into two sets associated respectively with the A' and A'' species. This reduces the size of the determinants and simplifies the calculation; it also allows use to be made of the vapor-phase band contours and the Raman polarizations to help assign the calculated frequencies to the correct experimental bands. This becomes an increasingly difficult problem as the size of the molecule increases and the symmetry diminishes. In addition, the use of symmetry coordinates permits the recognition and elimination of *redundant coordinates*. If there are more internal coordinates than normal modes of vibration, the system is overdefined, and redundant information is present. In this case there are 12 such redundant coordinates. When expressed in the Cartesian or internal coordinate systems, this redundant information is not separable, but in symmetry coordinates many of the redundancies become obvious on inspection An example is provided by S_{32} in Table II. This defines an in-plane bending

$$S_{32} = \chi_{46} + \epsilon_{43} + \epsilon_{44} \quad (5)$$

motion of the C–CO–C system in which all the angles at the central C atom increase simultaneously, which is clearly impossible. Of the 12 redundant coordinates, 6 local redundancies of this kind associated with the 6 carbon atoms of the ring are obvious and are noted in Table II. In the computer program the remaining 6 redundancies are identified in the process of normalization and are also eliminated. This leaves 45 symmetry coordinates corresponding to the 45 normal modes of vibration consistent with the $3N - 6$ formulation.[33]

In the final step of this part of the calculation, the **G** matrix is also transposed to symmetry coordinates to give $\mathcal{G}$ where

$$\mathcal{G} = UGU' \quad (6)$$

and the redundant elements are eliminated as for **S**.

(29) It is not feasible to avoid the use of matrix algebra. In these expressions **R** and $\dot{R}$ are single column matrices (vectors) of order $n = 3N - 6$ where N is the number of atoms in the molecule. **F** and **G** are symmetric square matrices of order n, composed of the coefficients F_{ij} and G_{ij}. For further discussions see ref 26, but note that in Mills' symbolism **M** denotes G^{-1} and differs from our use of **M**.
(30) $3N - 6$, $N = 17$.
(31) This follows from group theory. For the point group C_s there are $3m + 2m_0 - 3$ A' vibrations and $3m + m_0 - 3$ A'' vibrations, where m_0 is the number of atoms located in the symmetry plane and m the number of equivalent atom pairs lying off the plane: for cyclohexanone $m_0 = 5$ and $m = 6$.
(32) This excludes rotational and translational motions of the whole molecule which can be regarded as normal coordinates of zero frequency.
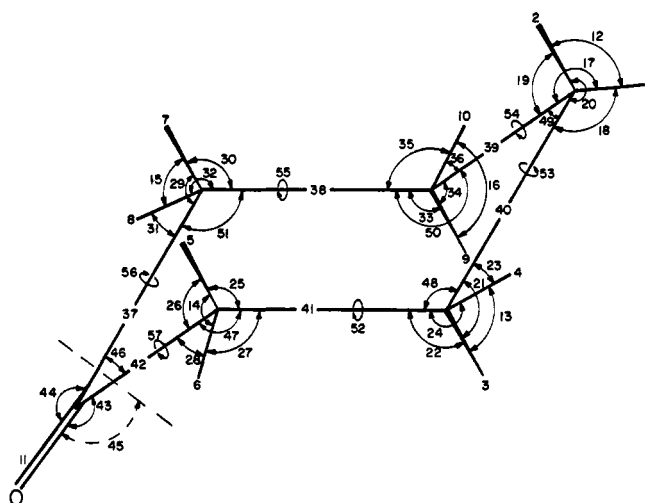(33) This is a somewhat oversimplified description of the redundancy problem; it is discussed more completely in ref 19.

Table II

Symmetry Coordinates for Cyclohexanone (Chair) (Not Normalized)

S_n	Internal coordinates involved[a]	Description[b]	S_n	Internal coordinates involved[a]	Description[b]
	A′ Species			**A″ Species**	
$S_1 = d_1 - d_2$		Asym γ CH stretch	$S_{33} = d_3 - d_4 - d_9 + d_{10}$		Asym β CH stretch
$S_2 = d_1 + d_2$		Sym γ CH stretch	$S_{34} = -d_3 - d_4 + d_9 + d_{10}$		Sym β CH stretch
$S_3 = -d_3 + d_4 - d_9 + d_{10}$		Asym β CH stretch	$S_{35} = -d_5 + d_6 + d_7 - d_8$		Asym α CH stretch
$S_4 = d_3 + d_4 + d_9 + d_{10}$		Sym β CH stretch	$S_{36} = -d_5 - d_6 + d_7 + d_8$		Sym α CH stretch
$S_5 = d_5 - d_6 + d_7 - d_8$		Asym α CH stretch	$S_{37} = -\delta_{13} + \delta_{16}$		β CH$_2$ scissor
$S_6 = d_5 + d_6 + d_7 + d_8$		Sym α CH stretch	$S_{38} = -\delta_{14} + \delta_{15}$		α CH$_2$ scissor
$S_7 = \delta_{12}$		γ CH$_2$ scissor	$S_{39} = \gamma_{17} - \gamma_{18} + \gamma_{19} - \gamma_{20}$		γ CH$_2$ wag
$S_8 = \delta_{13} + \delta_{16}$		β CH$_2$ scissor	$S_{40} = \gamma_{21} - \gamma_{22} + \gamma_{23} - \gamma_{24} +$		β CH$_2$ wag
$S_9 = \delta_{14} + \delta_{15}$		α CH$_2$ scissor	$\gamma_{33} - \gamma_{34} + \gamma_{35} - \gamma_{36}$		
$S_{10} = -\gamma_{21} + \gamma_{22} - \gamma_{23} + \gamma_{24} +$		β CH$_2$ wag	$S_{41} = \gamma_{25} - \gamma_{26} + \gamma_{27} - \gamma_{28} +$		α CH$_2$ wag
$\gamma_{33} - \gamma_{34} + \gamma_{35} - \gamma_{36}$			$\gamma_{29} - \gamma_{30} + \gamma_{31} - \gamma_{32}$		
$S_{11} = -\gamma_{25} + \gamma_{26} - \gamma_{27} + \gamma_{28} +$		α CH$_2$ wag	$S_{42} = \gamma_{17} - \gamma_{18} - \gamma_{19} + \gamma_{20}$		γ CH$_2$ twist
$\gamma_{29} - \gamma_{30} + \gamma_{31} - \gamma_{32}$			$S_{43} = \gamma_{21} - \gamma_{22} - \gamma_{23} + \gamma_{24} +$		β CH$_2$ twist
$S_{12} = -\gamma_{21} + \gamma_{22} + \gamma_{23} - \gamma_{24} +$		β CH$_2$ twist	$\gamma_{33} - \gamma_{34} - \gamma_{35} + \gamma_{36}$		
$\gamma_{33} - \gamma_{34} - \gamma_{35} + \gamma_{36}$			$S_{44} = \gamma_{25} - \gamma_{26} - \gamma_{27} + \gamma_{28} +$		α CH$_2$ twist
$S_{13} = -\gamma_{25} + \gamma_{26} + \gamma_{27} - \gamma_{28} +$		α CH$_2$ twist	$\gamma_{29} - \gamma_{30} - \gamma_{31} + \gamma_{32}$		
$\gamma_{29} - \gamma_{30} - \gamma_{31} + \gamma_{32}$			$S_{45} = -\gamma_{21} - \gamma_{22} + \gamma_{23} + \gamma_{24} +$		β CH$_2$ rock
$S_{14} = \gamma_{17} + \gamma_{18} - \gamma_{19} - \gamma_{20}$		γ CH$_2$ rock	$\gamma_{33} + \gamma_{34} - \gamma_{35} - \gamma_{36}$		
$S_{15} = \gamma_{21} + \gamma_{22} - \gamma_{23} - \gamma_{24} +$		β CH$_2$ rock	$S_{46} = -\gamma_{25} - \gamma_{26} + \gamma_{27} + \gamma_{28} +$		α CH$_2$ rock
$\gamma_{33} + \gamma_{34} - \gamma_{35} - \gamma_{36}$			$\gamma_{29} + \gamma_{30} - \gamma_{31} - \gamma_{32}$		
$S_{16} = \gamma_{25} + \gamma_{26} - \gamma_{27} - \gamma_{28} +$		α CH$_2$ rock	$S_{47} = r_{37} - r_{42}$		α C–C stretch
$\gamma_{29} + \gamma_{30} - \gamma_{31} - \gamma_{32}$			$S_{48} = r_{38} - r_{41}$		β C–C stretch
$S_{17} = v_{11}$		C=O stretch	$S_{49} = r_{39} - r_{40}$		γ C–C stretch
$S_{18} = r_{37} + r_{42}$		α C–C stretch	$S_{50} = \epsilon_{43} - \epsilon_{44}$		C=O bend in plane
$S_{19} = r_{38} + r_{41}$		β C–C stretch	$S_{51} = -\omega_{49} + \omega_{51}$		β CCC bend
$S_{20} = r_{39} + r_{40}$		γ C–C stretch	$S_{52} = -\omega_{48} + \omega_{50}$		α CCC bend
$S_{21} = \rho_{45}$		C=O bend out of plane	$S_{53} = \tau_{56} + \tau_{57}$		α-C(H$_2$)–C(O) torsion
$S_{22} = 2\chi_{46} - \epsilon_{43} - \epsilon_{44}$		CC(O)C bend	$S_{54} = \tau_{55} + \tau_{52}$		β-C(H$_2$)$_2$–C(H$_2$) torsion
$S_{23} = \omega_{47} + \omega_{51}$		α CCC bend	$S_{55} = \tau_{54} + \tau_{53}$		γ-C(H$_2$)–C(H$_2$) torsion
$S_{24} = \omega_{48} + \omega_{50}$		β CCC bend	$S_{56} = -\gamma_{21} - \gamma_{22} - \gamma_{23} - \gamma_{24} +$		Redundant
$S_{25} = \omega_{49}$		γ CCC bend	$\gamma_{33} + \gamma_{34} + \gamma_{35} + \gamma_{36}$		
$S_{26} = \tau_{56} - \tau_{57}$		α C(H$_2$)–C(O) torsion	$S_{57} = -\gamma_{25} - \gamma_{26} - \gamma_{27} - \gamma_{28} +$		Redundant
$S_{27} = \tau_{55} - \tau_{52}$		β C(H$_2$)–C(H$_2$) torsion	$\gamma_{29} + \gamma_{30} + \gamma_{31} + \gamma_{32}$		
$S_{28} = \tau_{54} - \tau_{53}$		γ C(H$_2$)–C(H$_2$) torsion			
$S_{29} = \gamma_{17} + \gamma_{18} + \gamma_{19} + \gamma_{20}$		Redundant			
$S_{30} = \gamma_{21} + \gamma_{22} + \gamma_{23} + \gamma_{24} +$		Redundant			
$\gamma_{33} + \gamma_{34} + \gamma_{35} + \gamma_{36}$					
$S_{31} = \gamma_{25} + \gamma_{26} + \gamma_{27} + \gamma_{28} +$		Redundant			
$\gamma_{29} + \gamma_{30} + \gamma_{31} + \gamma_{32}$					
$S_{32} = \chi_{46} + \epsilon_{43} + \epsilon_{44}$		Redundant			

[a] The $+$ and $-$ signs respectively identify an increase or decrease of the bond length or bond angle during the vibration. [b] All symmetry coordinates involving combinations of symmetrical internal coordinates yield an A′ type in-phase and an A″ type out-of-phase vibration for which the same description is used. Asym (antisymmetric) and Sym (symmetric) refer to the local site symmetry, not to the symmetry plane of the cyclohexanone molecule (*cf.* Table VIII).

C. POTENTIAL ENERGY, NORMAL COORDINATES, AND VIBRATIONAL FREQUENCIES

The potential energy must next be considered. In internal valence coordinates it is defined by the matrix of force constants **F**. In the general case this describes the interactive forces between all the atoms of the molecule. Expressed in symmetry coordinates it is defined by the stretch, bend, and torsional forces associated with the bond structure (the diagonal elements) and their mutual interactions (the off-diagonal elements). This matrix $\mathfrak{F}$ is related to F by

$$\mathfrak{F} = \mathbf{UFU'} \qquad (7)$$

and the expressions for the potential energy V are

$$2V = \mathbf{R'FR} \qquad (8)$$

in the respective coordinate systems (*cf.* eq 3).

Having obtained formal expressions for both the kinetic energy and the potential energy of the vibrational system, these can now be entered into the Hamiltonian equation to derive a set of energy levels (eigenvalues) which are related in a simple manner to the vibrational frequencies. Before doing this, however, it is necessary to perform yet another coordinate conversion to *normal coordinates* **Q**. These are characterized by the fact that in this coordinate system both T and V are diagonalized; *i.e.*, all the off-axis terms are zero.

The conversion to normal coordinates involves another transformation matrix $\mathfrak{L}$ where

$$2V = \mathbf{S'\mathfrak{F}S} \qquad (9)$$

$$\mathbf{S} = \mathfrak{L}\mathbf{Q} \qquad (10)$$

in terms of which

$$2V = Q'AQ \qquad (11)$$

$$2T = \dot{Q}'\dot{Q} \qquad (12)$$

where A is a diagonal matrix of the calculated eigenvalues and $\mathcal{L}$ is the eigenvector matrix which defines the normal coordinates in terms of the symmetry coordinates. $\dot{Q}_i = \delta Q_i/\delta t$ for the ith normal coordinate.

The Hamiltonian equation now becomes

$$\mathcal{G}\mathcal{F}\mathcal{L} = \mathcal{L}A \qquad (13)$$

and the wavenumber of the kth normal vibration is given by

$$\nu_k = (\Lambda_k N)^{1/2}/2\pi c \qquad (14)$$

where N is the Avogadro number and c is the velocity of light.

There are now available several well-tested computer programs which will perform the numerical computations associated with eq 1–14. These will display the various matrices on demand, and if the force field is known accurately eq 13 and 14 can be solved in this way for the eigenvalues and frequencies, respectively. The practical problem, however, is the inverse one; the frequencies are known from the spectroscopic measurements, and it is the force field which it is desired to evaluate. This cannot be done explicitly. The method adopted is to commence with a set of estimated force constants $\mathfrak{F}_0$, use eq 13 and 14 to compute the corresponding frequencies as eigenvalues, and minimize the squared error $\Delta\Lambda^2$ iteratively where

$$\Delta\Lambda = \sum_{i=1,n} [f(\Lambda_i{}^{\mathrm{obsd}} - \Lambda_i{}^{\mathrm{cacld}})] \qquad (15)$$

in which f is a suitably chosen weighting function.

This is a well-established procedure[34–36] known as *refinement*. The basic computer program for large polyatomic molecules FPERT was written by Snyder and Schachtschneider[37] in 1962. There are more recent variants[38,39] and our own modification is included in ref 19.

D. POTENTIAL ENERGY DISTRIBUTION FUNCTION

Given a defined molecular configuration and an optimized eigenvalue–frequency fit, the refined force constants comprise the primary end-product of the normal coordinate calculation. For small molecules, especially where the complete (general) force field has been used, the next logical task for the molecular spectroscopist is to use this information to interpret the forces stabilizing the structure and relate them to the bond character in terms of molecular orbitals or some alternative bond structure theory. In this he is restrained by the knowledge that the refinement process leads only to one of several possible sets of force constants, and he is circumspect about attaching too much significance to any interpretation he may be tempted to make.[4]

It would, however, be an error of judgement to apply the same rigid criteria to the much cruder attempts to use normal coordinate analysis to interpret the spectra of complex molecules. It must be recognized in the first place that in the choice of the initial selective valence force field, the chemist who applies normal coordinate analysis to complex molecules has already surrendered the absolute significance of the force constants quite apart from the multiplicity of the convergent paths during refinement. It is therefore necessary to seek some other numerical output from the computation that is less sensitive to the choice of the initial force field and can be related more directly to the empirical group vibration.

This purpose may be served by the *potential energy distribution coefficient* $E_{\mathrm{p}(i)}$ where

$$E_{\mathrm{p}(i)} = \mathcal{L}_{ki}{}^2 \mathfrak{F}_{kk} \cdot (100/\lambda_i) \qquad (16)$$

in which λ_i is the eigenvalue of the ith normal vibration, $\mathfrak{F}_{kk}$ the value of the kth symmetrized diagonal force constant, and $\mathcal{L}_{ki}$ an element of the normal coordinate transformation matrix.[40]

$E_{\mathrm{p}(i)}$ quantifies the distribution of the potential energy of the vibrational mode among the symmetry or internal coordinates. For a "pure" C=O stretch group frequency the potential energy of the mode would be located entirely in the C=O stretch coordinate (v of Figure 2). It will be seen later that in cyclohexanone only about 70% of the potential energy of the mode near 1715 cm^{-1} is so localized and at least four other internal coordinates participate significantly in the motion. In a series of calculations in which the refined value of the C=O stretch force constant ranged from 9.2 to 10.6 mdyn Å^{-1}, this proportionality remained within ±9%, though the nature of the selective force field and the number of nonzero force constants varied extensively. The same stable behavior of $E_{\mathrm{p}(i)}$ is observed also in the computations of Cossee and Schachtschneider for simple aldehydes and ketones.[41] $E_{\mathrm{p}(i)}$ has the additional feature that it can be displayed graphically as a vector in a form which clearly indicates its significance as a means of quantifying the group frequency.[42]

Unless sufficient attention is given to the potential energy distribution in establishing refined valence force fields, serious errors can arise. This has been emphasized[43–45] but papers still appear in which the potential energy distribution is not reported. Without this information it is very difficult to assess the relevance of the computations.

E. CHOICE OF THE INITIAL FORCE FIELD

A complete description of a general force field taking account of all interatomic interactions requires $n(n + 1)/2$ force con-

(34) D. E. Mann, T. Shimanouchi, J. H. Meal, and L. Fano, *J. Chem. Phys.*, 27, 43 (1957).

(35) J. Overend and J. R. Scherer, *ibid.*, 32, 1289, 1296 (1960).

(36) J. Aldous and I. M. Mills, *Spectrochim. Acta*, 18, 1073 (1962).

(37) J. H. Schachtschneider, Technical Report, No. 57-65, Shell Development Co., Emeryville, Calif., 1966.

(38) F. C. Curtis, "Computer Program for Calculating Vibrational Frequencies and Force Constants of Simple Polyatomic Molecules," Rocketdyne Corp., Publication No. R-6768, Oct. 1966.

(39) T. Shimanouchi, "Computer Programs for Normal Coordinate Treatment of Polyatomic Molecules," Department of Chemistry, Faculty of Science, University of Tokyo, July 1968.

(40) More correctly we should write $E_{\mathrm{p}(i,k)}$ in place of $E_{\mathrm{p}(i)}$, but the k coefficient is always clear from the context (*cf.* columns 8–11 of Tables IVA–D where it is identified by the internal valence coordinate symbols of Figure 2). In later work we have also dropped the i coefficient since this is needed only to cite back to the listing order in the eigenvalue column matrix; this is trivial in discussion where the eigenvalues are better identified by ν_{calcd}.

Some authors refer to $E_{\mathrm{p}(i)}$ as PED, an acronym for Potential Energy Distribution. For other examples of its use to characterize acceptable force fields, see C. Di Lauro, S. Califano, and G. Adembri, *J. Mol. Struct.*, 2, 173 (1968); A. Rogstag, P. Klaboe, B. N. Cyvin, S. J. Cyvin, and D. H. Christensen, *Spectrochim. Acta, Part A*, 28, 111 (1972).

(41) P. Cossee and J. H. Schachtschneider, *J. Chem. Phys.*, 44, 97 (1966).

(42) See Figure 8 of ref 41.

(43) C. D. Needham and J. Overend, *Spectrochim. Acta*, 22, 1385 (1966).

(44) J. M. Freeman and T. Henshall, *J. Mol. Spectrosc.*, 25, 101 (1968).

(45) J. M. Freeman and P. J. Robinson, *Can. J. Chem.*, 49, 2533 (1971).

stants, where n is the number of internal coordinates. This amounts to 1653 for cyclohexanone, but this is a mathematic abstraction, since the forces between remote atoms are negligible in our approximation and many of these terms will be zero. We have achieved an acceptable force field with the 44 defined constants listed in Table III; these were derived by an extensive series of computations, starting with an initial set of 59 constants from which 15 were subsequently eliminated. It is in the selection of these defined force constants and in the choice of their initial values that the second element of chemical intuition is injected into the calculations.

If the initial force field is poorly chosen, the refinement program may converge to chemically unrealistic force constants, or not converge at all. The best approach is to transfer constants from simpler related molecules. This will clearly become more facile as more refined force constant data become available; thus rapid convergence is obtained for cyclopentanone using as input the refined constants from cyclohexanone.[20] For the C_β-C_γ-C_β part of cyclohexanone, the generalized values for aliphatic and alicyclic hydrocarbons established by Snyder and Schachtschneider[13] were used, and for the C_α-CO-C_α structure the values of Cossee and Schachtschneider[41] were transferred from acetone. This initial set is listed in column 5 of Table III.[46]

The 20 diagonal force constants comprise the core of the valence force field. In the C_α-C_β-C_γ-C_β-C_α moiety all the C-C constants of the same type were initially set equal, as were the C-H constants, but provision was made for all but two to vary during the refinement depending on their association with the α, β, or γ position. Two of the bend constants $H_{\omega(\beta\gamma)}$ and $H_{\tau(\beta\gamma)}$ associated with the skeletal CCC bend (no. 15) and the CC torsion (no. 20) were fixed in the sense that no difference was allowed to develop between those involving the β and γ positions. In addition 24 off-diagonal constants were included. These allow for interaction between certain coordinates sharing at least one common atom.

The interaction constants are unquestionably helpful in obtaining a better fit with the experimental frequencies, but their physical meaning is difficult to conceptualize. In simple molecules they have been discussed by Thompson and Linnett[47] in terms of changes in the bond hybridization during the vibration. This is clearly a relevant factor, but in complex molecules other influences must also be considered such as van der Waals and electrostatic forces between nonbonded atoms. In large molecules where their form and number is artificially constrained by the imposition of a selective force field, it is perhaps advisable to regard them as semiempirical parameters analogous to those used in quantum chemistry, as, for example, in Hückel and self-consistent field calculations to improve the fit between calculated and observed electronic energy levels of molecules. As information accumulates on more molecules of the same general type, it may well be that systematic trends will become evident so that their relative values, if not their absolute values, will aid our understanding of the molecular force field. Readers wishing to pursue this further are directed to the writings of Califano[15] and Shimanouchi[48] and the references cited therein.

(46) The conventional symbolism is used: K designates a bond stretch constant, H an angle bend constant, and F an interaction constant. The first subscript identifies the type of internal coordinate and the parenthesized subscript the skeletal atom involved. Thus $K_{d(\alpha)}$ is the stretch force constant for a C-H bond on the α carbon atom. Axial and equatorial C-H bonds are not differentiated.

(47) H. W. Thompson and J. W. Linnett, *J. Chem. Soc.*, 1384 (1937).

(48) See pp 291-297 of ref 22.

Table III

Valence Force Constants for Cyclohexanone[a]

No.	Symbol	Coordinates involved	Common atoms	Starting value	Refined value
		Direct Force Constants			
		Stretch			
1	$K_{d(\alpha)}$	C-H		4.554	4.685
2	$K_{d(\beta)}$	C-H		4.554	4.610
3	$K_{d(\gamma)}$	C-H		4.554	4.533
4	K_v	C=O		9.723	9.652
5	$K_{r(\alpha)}$	C-C		4.387	4.564
6	$K_{r(\beta)}$	C-C		4.387	4.186
7	$K_{r(\gamma)}$	C-C		4.387	4.136
		Bend			
8	$H_{\delta(\alpha)}$	∠HCH		0.55	0.554
9	$H_{\delta(\beta)}$	∠HCH		0.55	0.567
10	$H_{\delta(\gamma)}$	∠HCH		0.55	0.579
11	$H_{\gamma(\alpha)}$	∠HCC		0.656	0.628
12	$H_{\gamma(\beta)}$	∠HCC		0.656	0.657
13	$H_{\gamma(\gamma)}$	∠HCC		0.656	0.679
14	$H_{\omega(\alpha)}$	∠CCC		1.13	1.068
15	$H_{\omega(\beta\gamma)}$	∠CCC		1.13	1.024
16	H_χ	∠CCC		1.65	1.111
17	H_ϵ	∠CCO		1.001	0.919
18	H_ρ	∠C-CO-C		0.217	0.534
19	$H_{\tau(\alpha)}$	∠CC-CC		0.024	0.008
20	$H_{\tau(\beta\gamma)}$	∠CC-CC		0.024	0.093
		Interaction Constants[b]			
		Stretch-Stretch			
21	$F_{\alpha,\alpha}$	C-H, C-H	C	0.006	0.006
22	$F_{r,r}$	C-C, C-C	C	0.101	0.101
23	$F_{r(\alpha),v}$	C-C, C=O	C	0.0	0.0
		Stretch-Bend			
24	$F_{r,\gamma}$	C-C, ∠HCC	C-C	0.328	0.328
25	$F_{r',\gamma}$	C-C, ∠HCC	C	0.079	0.079
26	$F_{r,\omega}$	C-C, ∠CCC	C-C	0.417	0.417
27	$F_{r(\alpha),\epsilon}$	C-C, ∠CCO	C-C	0.417	0.417
28	$F_{r(\alpha),\chi}$	C-C, ∠CCC	C-C	0.417	0.417
29	$F_{v,\chi}$	C=O, ∠CCC	C	0.0	0.0
		Bend-Bend			
30	$F_{\delta,\gamma}$	∠HCC, ∠HCC	H-C	0.0	0.0
31	$F_{\gamma,\gamma}$	∠HCC, ∠HCC	C-C	−0.021	−0.021
32	$F_{\gamma',\gamma}$	∠HCC, ∠HCC	H-C	0.012	0.012
33	$F^t_{\gamma,\gamma}$	∠HCC, ∠HCC	C-C	0.127	0.127
34	$F^g_{\gamma,\gamma}$	∠HCC, ∠HCC	C-C	−0.005	−0.005
35	$F_{\gamma,\omega}$	∠HCC, ∠CCC	C-C	−0.031	−0.031
36	$F^t_{\gamma,\omega}$	∠HCC, ∠CCC	C-C	0.049	0.049
37	$F^g_{\gamma,\omega}$	∠HCC, ∠CCC	C-C	−0.052	−0.052
38	$F^t_{\gamma(\alpha),\chi}$	∠HCC, ∠CCC	C-C	0.0	0.0
39	$F^g_{\gamma(\alpha),\chi}$	∠HCC, ∠CCC	C-C	0.0	0.0
40	$F^{cis}_{\gamma(\alpha),\epsilon}$	∠HCC, ∠CCO	C-C	0.0	0.0
41	$F^g_{\gamma(\alpha),\epsilon}$	∠HCC, ∠CCO	C-C	0.0	0.0
42	$F_{\omega,\omega}$	∠CCC, ∠CCC	C-C	0.0	0.0
43	$F_{\omega,\chi}$	∠CCC, ∠CCC	C-C	0.0	0.0
44	$F_{\tau(\alpha),\rho}$	∠CC-CC, ∠C-CO-C	C-C-C	0.0	0.0

[a] The force constant units are: stretch, mdyn Å^{-1} (10^2 N m^{-1}); bend, mdyn Å (10^{-18} N m); stretch-stretch, mdyn Å^{-1}; stretch-bend, mdyn (10^{-8} N); bend-bend, mdyn Å. The equivalents in SI units are given in parentheses; the bending constants are unscaled (see p 178 of ref 26); angular measurements are in radians. [b] The interaction constants were not refined. Some were fixed at 0.0, either because they were strongly correlated (no. 23, 29) or because their values remained consistently below 0.02 (no. 30, 38-44). Though fixed at 0.0, they still influence the computations (see ref 19).
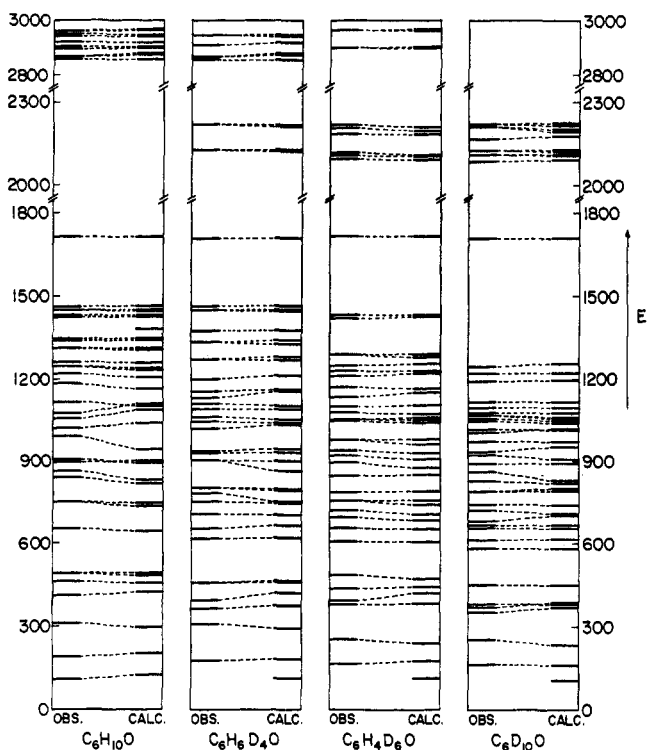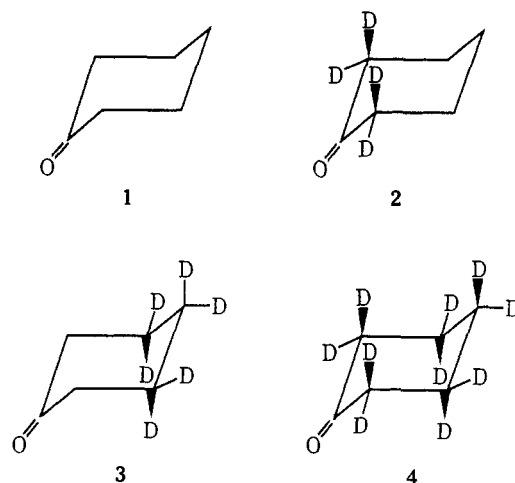
Figure 4. Energy level diagrams: comparison of the observed and calculated frequencies of the four isotopic species.

For large molecules the process of refinement cannot be allowed to proceed in a totally automatic manner under complete computer control. Human intervention is necessary to guide the computation toward a chemically reasonable solution. Such manipulation might be construed as unscientific, but the process is not arbitrary; it is not difficult to recognize when the system is converging to a patently false solution, even though there may be satisfactory agreement between the computed and measured frequencies. In the initial stages of the refinement, pairs of force constants may exhibit strong correlations as a result of which they drift toward unreasonably high or low values.[49] To control this the program permits preselected constants to be held fixed during the initial stages of the refinement and to be released later when convergence will progress to a chemically reasonable solution.

The appropriateness of the initial force field can be tested by substituting the initial force constants $\mathcal{F}_0$ into eq 13 and comparing the computed and experimental frequencies. The final set of refined force constants obtained for cyclohexanone is listed in the last column of Table III. The analysis was performed simultaneously on cyclohexanone (1) and the three deuterated species 2-4 which have the same symmetry. This set provided 180 frequencies for the evaluation of 20 adjustable force constants. The average frequency error is 1.3% if the frequencies are weighted reciprocally.[19] This corresponds to an average error of ±4.6 cm⁻¹. The results are summarized in the energy level diagrams shown in Figure 4 which permit easy comparison among the four isotopic species.

Force constant calculations on cyclohexanone have also been made recently by Rey-Lafon and Forel[50] with whom we have exchanged information during the course of these investigations. Their computations were based on structures 1 and 2 only, using 27 refined and 3 fixed force constants to fit 70 experimental frequencies. There is agreement on the vibrational assignments and a general consistence concerning the interpretation of the vibrational modes, though a detailed comparison is not possible because of their use of a simpler set of internal coordinates.

A note of caution is in order concerning the direct comparison of force constants for the same molecule obtained by different investigators using different restraints in the refinement process. Valence bond stretch, angle bend, and torsional force constants, as normally evaluated at present, can be strongly dependent on the precise manner in which they are defined. In a sense the individual valence force constants measure the amount of energy required to distort the molecule from its equilibrium configuration in a physically impossible way, by dealing with very small isolated fragments of the molecule e.g., the deformation of an individual HCC angle in a methylene group. It is clear, however, that one HCC angle cannot be altered without affecting other angles; in our treatment this shows up in the appropriate off-axis terms. An alternative, very appealing to the chemist, is to establish "group force constants" (known also as local symmetry force field (LSFF) constants) for larger vibrating structural systems such as methylene rocks or wags. The force field set up for cyclohexanone by Rey-Lafon and Forel makes some use of this approach, but it has not yet been applied to a sufficient variety of large molecules to permit assessment of the transferability of such group force constants; for further discussion see ref 51-54.

III. Spectral Measurements

Cyclohexanone (1) and cyclohexanone-d_{10} (4) are commercially available compounds, from which the partially deuterated compounds were prepared in our laboratory by exchange at the reactive α positions.

(49) The force constant pairs 4–16, 6–7, 12–13, 14–15, 18–19 of Table III exemplify this in cyclohexanone. One of each pair was fixed initially and released later. The degree of interaction between all the force constants is computed by the FPERT program and displayed in a correlation matrix. It is essential that this be analyzed carefully during the refinement. It is considered in more detail in ref 19.

(50) M. Rey-Lafon and M.-T. Forel, *Bull. Soc. Chim. Fr.*, 384 (1971).
(51) J. L. Duncan and I. M. Mills, *Spectrochim. Acta*, 20, 523, 1089 (1964).
(52) J. L. Duncan and G. R. Burns, *J. Mol. Spectrosc.*, 30, 253 (1969).
(53) See pp 287–291 of ref 22.
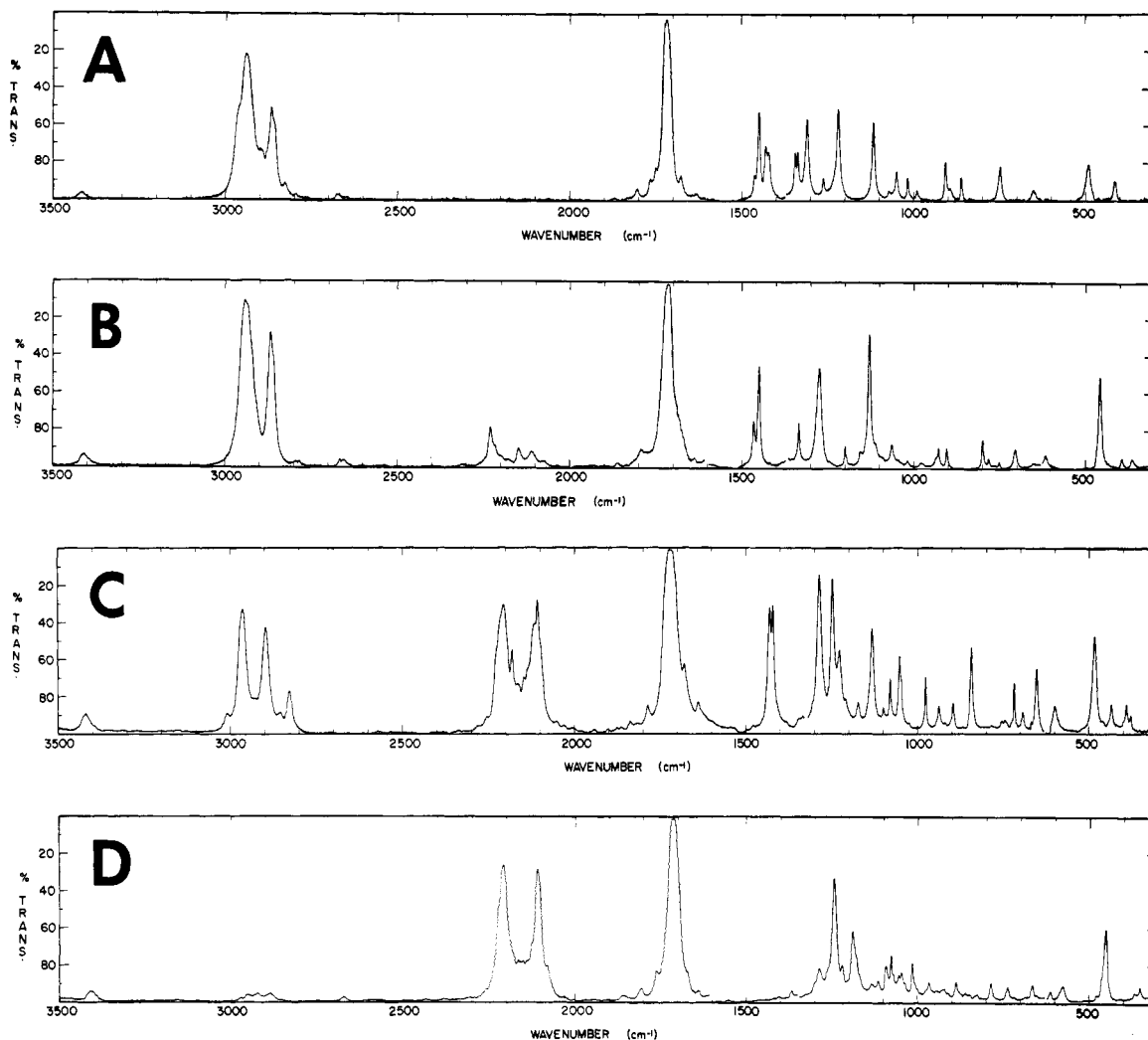(54) J. E. Bertie and M. G. Norton, *Can. J. Chem.*, 49, 2229 (1971).

Figure 5. Infrared spectra in solution: solvent CCl_4 (4000–1380/630–240 cm^{-1}); CS_2 (1380–630 cm^{-1}). Path length 1 mm. (A) $C_6H_{10}O$, (B) $C_6H_6D_4O$, (C) $C_6H_4D_6O$, (D) $C_6D_{10}O$.

Cyclohexanone (**1**). Reagent grade material was purified by vapor-phase chromatography and repeated fractional distillation *in vacuo*.

Cyclohexanone-α,α,α',α'-d₄ (**2**). Cyclohexanone (5 ml), deuterium oxide (75 ml, 99.97%), and potassium carbonate (0.5 g) were heated under reflux for 52 hr; the cooled product was saturated with sodium chloride and extracted twice with ether (200 ml). After drying over sodium sulfate, the ether was removed by gentle warming and the ketone distilled at 155.6°, yield 2.5 ml. Analysis by mass spectrometry gave $C_6H_6D_4O$, 94.1%; $C_6H_7D_3O$, 4.5%; $C_6H_5D_5O$, 1.4%.

Cyclohexanone-β,β,β',β',γ,γ'-d₆ (**3**) was prepared by dedeuteration of **4** using the same exchange reaction conditions as for **2** with water replacing deuterium oxide. Analysis by mass spectrometry gave $C_6H_4D_6O$, 77.5%; $C_6H_5D_5O$, 7.4%; $C_6H_3D_7O$, 7.1%; $C_6H_2D_8O$, 6.5%; $C_6H_6D_4O$, 1.2%.

Cyclohexanone-d₁₀ (**4**) was purchased from Merck Sharpe and Dohme, Ltd. Analysis by mass spectrometry gave $C_6D_{10}O$, 78.1%; C_6HD_9O, 18.9%; $C_6H_2D_8O$, 2.3%.

The isotopic contents were also checked by proton magnetic resonance spectrometry which gave results consistent with the mass spectral data. All samples were single peaked on vapor-phase chromatographic analysis.

The infrared spectra were measured on the pure liquids and

on solutions in carbon tetrachloride, tetrachloroethylene, and carbon disulfide over the combined range 4000–260 cm^{-1} in 1-mm cells thermostated at 25 ± 1°. A Perkin-Elmer Model 521 spectrophotometer was used with the output digitally encoded at 0.5-cm^{-1} intervals on punched paper tape. These raw data were processed by the method used routinely in these laboratories.[55,56] This applies corrections for baseline nonlinearity, wavenumber and intensity calibration errors, and spectral slit convolution. The wavenumber scale was calibrated with doped indene.[57,58] Commercial Spectroquality solvents were used, checked by vapor-phase chromatography; the ranges were carbon tetrachloride, 4000–1350, 630–260 cm^{-1}; tetrachlorethylene, 1650–1350 cm^{-1}; carbon disulfide, 1350–630 cm^{-1}. The spectral slit schedules were 4000–2000 cm^{-1}, $\Delta\nu_{1/2} = 2.5$ cm^{-1}; 2000–630 cm^{-1}, $\Delta\nu_{1/2} = 1.5$ cm^{-1}; 630–260 cm^{-1}, $\Delta\nu_{1/2} = 2.5$ cm^{-1}. The positions of the band maxima were evaluated by our computer program PC-120[59] which is incorporated into the general data reduction routine.

(55) R. N. Jones, *J. Jap. Chem.*, **21**, 609 (1967).
(56) R. N. Jones, *Pure Appl. Chem.*, **18**, 303 (1969).
(57) "Tables of Wavenumbers for the Calibration of Infrared Spectrometers," *ibid.*, **1**, 537 (1961).
(58) R. N. Jones and A. Nadeau, *Spectrochim. Acta*, **20**, 1175 (1964).
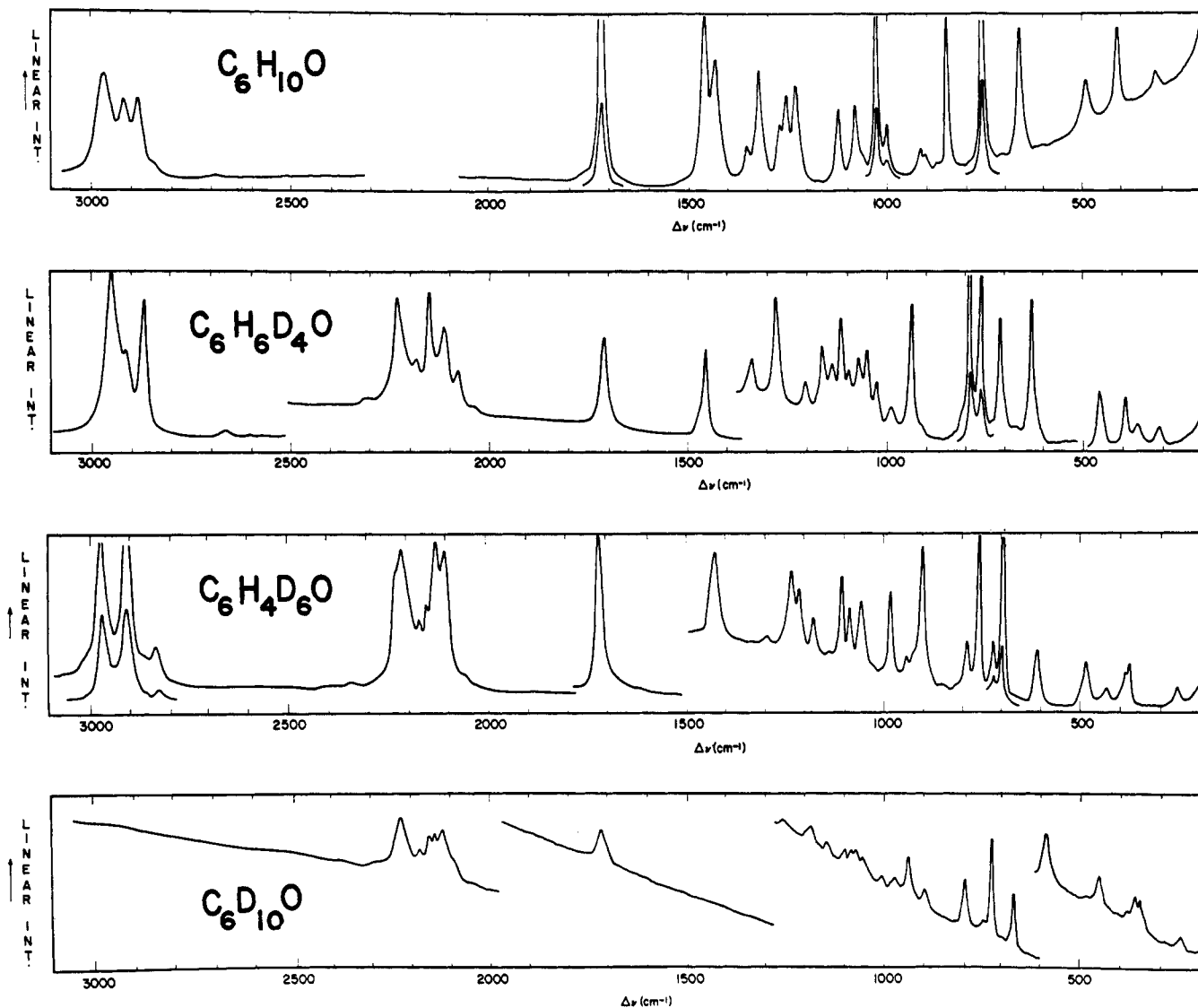(59) R. N. Jones, *Appl. Opt.*, **8**, 597 (1969).

Figure 6. Raman spectra of the pure liquids measured with 4358-Å Hg arc excitation without polarizers.

The peak positions are listed in Tables IVA–IVD for the measurements on the pure liquids; the estimated accuracy is ± 0.5 cm^{-1} on the fully resolved peaks. The computer plots of the processed spectra are shown in Figure 5. The computer analysis does not locate the positions of the inflections which were estimated visually from the curves.

The Raman spectra of the pure liquids were measured on a Cary Model 81 spectrophotometer using 4358-Å mercury radiation from a Toronto arc source. Spectra were also obtained from 1 and 2 with a Spectra-Physics Model 125 spectrophotometer using a 50-mW helium–neon laser source. The Hg arc and laser source measurements are listed separately in Tables IVA and IVB and the curves are shown in Figure 6. The polarization ratios in Tables IVA and IVB were obtained with the laser source using a rectangular cell. Those recorded in Tables IVC and IVD were measured on the Hg arc spectrophotometer using a capillary cell; their higher values are attributed to the less satisfactory geometry of this optical system.[60]

In comparing calculated and experimental frequencies, the averages of the Raman and infrared measurements were used. No corrections were applied for solvent displacement effects, though ideally the values for the vapor phase should be compared with the theoretical values. Except for the most polar vibrations (notably the C=O stretch band), this solvent shift would not be expected to exceed 2–3 cm^{-1}, and a somewhat dubious correction is not justified when considered in relation to other sources of error and approximation inherent in the computations. Notable among these is the assumption of the harmonic force field.

IV. Discussion

The hazards of probing too deeply into the significance of the *absolute* values of the refined force constants have already been stressed; their main importance is as input values for transfer to other molecules. The *relative* values may be more significant; the perturbation introduced by the sp^2 carbonyl bond on the C–H and C–C stretch constants and on the C–C–H bend constants can be observed as far as the γ position. The starting values of K_d, K_r, H_γ, H_δ, H_ω, and H_τ were not

(60) R. N. Jones, J. B. DiGiorgio, J. J. Elliott, and G. A. A. Nonnenmacher, *J. Org. Chem.*, **30**, 1822 (1965).

Table IVA

Cyclohexanone (1)

No.	Sym	Calcd ν, cm⁻¹	Ir ν, cm⁻¹	Raman Hg arc	Raman Laser	ρ	Potential energy distribution coefficients				Mode type
1	A'	121	(112)ᶜ	107	105 m		$\omega_\alpha(32)$	$\tau_{\beta\gamma}(13)$	$\rho(13)$	$\chi(12)$	DF
2	A''	200	(190)ᵉ	186	189 m	0.68	$\tau_{\beta\gamma}(46)$	$\omega_{\beta\gamma}(21)$	$\omega_\alpha(15)$		ZF
3	A'	295	(315)ᵉ	312	313 m	0.39	$\omega_{\beta\gamma}(34)$	$\tau_{\beta\gamma}(33)$	$\omega_\alpha(10)$	$\gamma_\beta(10)$	ZF
4	A'	421	410 m	409	411 s	0.71	$\chi(32)$	$\omega_{\beta\gamma}(21)$	$\epsilon(13)$	$\rho(6)$	DF
5	A''	452	460 vw				$\omega_{\gamma\beta}(34)$	$\omega_\alpha(28)$	$\gamma_\alpha(15)$	$\gamma_\beta(12)$	DF
6	A''	484	490 s	490	491 m	0.77	$\epsilon(68)$	$\omega_\alpha(11)$			GF
7	A'	488					$\omega_{\beta\gamma}(36)$	$\gamma_\alpha(21)$	$\gamma_\beta(18)$	$\rho(19)$	DF
8	A'	643	652 m	653	655 vs	0.06	$\rho(32)$	$r_\beta(14)$	$r_\alpha(11)$	$\gamma_\beta(11)$	DF
9	A'	733	748 s	750	752 vs	0.06	$r_\alpha(47)$	$\gamma_\beta(17)$	$r_\gamma(14)$		DF
10	A''	745					$\gamma_\beta(42)$	$\gamma_\alpha(39)$	$r_\gamma(9)$		ZF
11	A'	815	838 vw	839	841 vs	0.05	$r_\gamma(51)$	$r_\alpha(13)$	$r_\beta(12)$	$\gamma_\gamma(11)$	DF
12	A'	830	861 m		865 w		$\gamma_\alpha(40)$	$\gamma_\gamma(26)$	$\gamma_\beta(19)$	$\rho(10)$	ZF
13	A''	901	907 s	908	911 w	0.78	$\gamma_\alpha(30)$	$\gamma_\beta(30)$	$r_\beta(22)$	$\gamma_\gamma(12)$	DF
14	A''	892	894 m	894	896 w	0.78	$r_\beta(35)$	$\gamma_\beta(16)$	$\gamma_\alpha(17)$	$r_\gamma(15)$	DF
15	A'	942	990 w	993	993 m	0.72	$\omega_{\beta\gamma}(17)$	$\omega_\alpha(15)$	$\gamma_\alpha(15)$	$\gamma_\beta(12)$	DF
16	A'	1039	1018 m	1017	1019 vs	0.74	$r_\beta(34)$	$\gamma_\beta(16)$	$\gamma_\alpha(12)$	$r_\gamma(10)$	DF
17	A''	1086	1049 m	1055	1057 w*		$r_\gamma(46)$	$r_\beta(20)$			ZF
18	A''	1111	1072 w	1072	1075 s	0.75	$\gamma_\alpha(49)$	$\gamma_\beta(40)$	$\gamma_\gamma(15)$		ZF
19	A'	1102	1117 vs	1114	1116 s	0.28	$\gamma_\alpha(34)$	$\gamma_\beta(24)$			DF
20	A''	1163	1185 w*				$\gamma_\beta(50)$	$r_\alpha(22)$	$\gamma_\gamma(16)$	$\gamma_\alpha(15)$	ZF
21	A'	1205	1220 vs	1222	1224 s	0.78	$\gamma_\alpha(69)$	$r_\beta(11)$	$\gamma_\beta(11)$		GF
22	A''	1234	1247 m*	1246	1248 s	0.83	$\gamma_\alpha(45)$	$r_\alpha(34)$	$\epsilon(14)$		ZF
23	A'	1238					$\gamma_\beta(52)$	$\gamma_\alpha(34)$			ZF
24	A''	1259	1263 m	1263	1266 m	0.79	$\gamma_\gamma(40)$	$\gamma_\alpha(37)$	$\gamma_\beta(12)$		ZF
25	A'	1307	1311 vs	1315	1316 s	0.79	$\gamma_\alpha(49)$	$\gamma_\beta(47)$			ZF
26	A''	1315					$\gamma_\alpha(46)$	$r_\alpha(31)$	$\gamma_\beta(26)$		ZF
27	A''	1343	1338 s				$\gamma_\gamma(59)$	$\gamma_\beta(38)$			ZF
28	A'	1344	1346 s	1347	1348 m	0.70	$\gamma_\beta(73)$	$\gamma_\alpha(16)$	$r_\beta(13)$		GF
29	A''	1383					$\gamma_\beta(42)$	$\gamma_\beta(35)$	$r_\gamma(19)$		ZF
30	A'	1429	1421 s	1423	1424 s		$\delta_\alpha(80)$	$\gamma_\alpha(19)$			GF
31	A''	1430	1429 s	1429	1429 s*	0.82	$\delta_\alpha(79)$	$\gamma_\alpha(19)$			GF
32	A'	1449	1449 vs	1451	1452 vs	0.82	$\delta_\beta(76)$	$\gamma_\beta(19)$			GF
33	A''	1448					$\delta_\beta(80)$	$\gamma_\beta(20)$			GF
34	A'	1466	1462 m	1463	1464 m*		$\delta_\gamma(78)$	$\gamma_\gamma(20)$			GF
35	A'	1715	1718 vvs	1710	1709 vs	0.35	$v(75)$	$r_\alpha(13)$	$\chi(6)$	$\gamma_\alpha(5)$	GF
36	A'	2853	2859 s*			0.10	$d_\gamma(99)$				GF
37	A''	2877	2867 s				$d_\beta(99)$				GF
38	A'	2878		2864	2865 vs	0.16	$d_\beta(99)$				GF
39	A''	2900	2894 s				$d_\alpha(99)$				GF
40	A'	2901		2900	2899 vs	0.25	$d_\alpha(99)$				GF
41	A'	2918	2920 s*				$d_\gamma(96)$				GF
42	A''	2941	2940 vs				$d_\beta(98)$				GF
43	A'	2944		2949	2950 vs	0.31	$d_\beta(94)$				GF
44	A''	2965	2961 s*				$d_\alpha(98)$				GF
45	A'	2967					$d_\alpha(97)$				GF

ᵃ GF = group frequency (see p 450), ZF = zone frequency, DF = delocalized frequency. ᵇ An asterisk denotes an inflection. ᶜ These are recent measurements on a Perkin-Elmer Model 180 spectrophotometer made after the completion of the numerical analysis.

differentiated on the α, β, and γ carbon atoms (Table III, column 5), but systematic changes evolve during the refinement, making $K_{d(\alpha)} > K_{d(\beta)} > K_{d(\gamma)}$; $K_{r(\alpha)} > K_{r(\beta)} > K_{r(\gamma)}$; $H_{\gamma(\alpha)} < H_{\gamma(\beta)} < H_{\gamma(\gamma)}$; $H_{\delta(\alpha)} < H_{\delta(\beta)} < H_{\delta(\gamma)}$; $H_{\omega(\alpha)} > H_{\omega(\beta\gamma)}$ and $H_{\tau(\alpha)} < H_{\tau(\beta\gamma)}$. The same trend was observed through many sets of calculations in which both the numerical values of the input force constants and the choice of the nonzero off-diagonal constants was varied. The effect on the α position correlates with the recognized frequency displacement of the α-CH₂ scissor group frequency (cf. Table VII).

The contributions of the principal internal coordinates to the normal modes are listed in column 6 of Tables IVA–IVD.

The figures in parentheses are the potential energy distribution coefficients ($E_{p(i)}$). These approximate to percentages, but the correspondence is not exact; some of the off-diagonal terms may induce small negative coefficients, in which case the total contributions from the positive terms can exceed 100. With occasional exceptions we have included in Table IVA–IVD only those diagonal force constants associated with internal coordinates for which $E_{p(i)} > 10$; these are the main contributors and their proportionality is less sensitive to the choice of the force field than that of the minor contributors. The analysis of the complete potential energy distribution matrix is one of the means used to guide the com-

Table IVB

Cyclohexanone-$\alpha,\alpha,\alpha',\alpha'$-$d_4$ (2)

No.	Sym	ν, cm⁻¹	Ir ν, cm⁻¹ᵃ	Raman, Δv, cm⁻¹ Hg arc	Laserᵃ	ρ	Potential energy distribution coefficients				Mode type
1	A'	114	(104)ᵇ		101		$\omega_\alpha(32)$	$\tau_{\beta\gamma}(13)$	$\chi(13)$	$\rho(12)$	DF
2	A''	181	(174)ᵇ		175		$\tau_{\beta\gamma}(45)$	$\omega_{\beta\gamma}(24)$	$\omega_\alpha(13)$		ZF
3	A'	288	(307)ᵇ	306	308 m		$\omega_{\beta\gamma}(36)$	$\tau_{\beta\gamma}(35)$			ZF
4	A'	374	360 m	362	361 m		$\gamma_\alpha(28)$	$\chi(26)$	$\rho(20)$	$\epsilon(11)$	DF
5	A''	419	390 m	390	392 m	0.85	$\gamma_\alpha(25)$	$\omega_{\beta\gamma}(22)$	$\omega_\alpha(22)$	$\epsilon(16)$	DF
6	A'	454	454 vs	454	455 s		$\omega_{\rho\gamma}(48)$	$\gamma_\beta(22)$	$\gamma_\alpha(13)$	$\gamma_\gamma(13)$	ZF
7	A''	463					$\epsilon(55)$	$\omega_\alpha(20)$			ZF
8	A'	619	616 m	614	614 vs	0.06	$\rho(24)$	$r_\alpha(16)$	$\gamma_\alpha(14)$	$\gamma_\beta(12)$	DF
9	A''	663	652 w				$\gamma_\alpha(53)$	$\gamma_\beta(16)$			ZF
10	A'	701	704 m	708	709 s	0.20	$r_\alpha(46)$	$\gamma_\alpha(12)$	$\gamma_\beta(12)$		DF
11	A'	745	751 w	754	754 vs	0.13	$\gamma_\alpha(41)$	$\gamma_\gamma(25)$	$\gamma_\beta(14)$	$r_\beta(10)$	ZF
12	A'	747	782 m	784	786 vs	0.07	$r_\gamma(42)$	$\gamma_\alpha(33)$	$r_\beta(13)$		ZF
13	A''	790	799 s	805	803 m*		$\gamma_\alpha(54)$	$\gamma_\beta(28)$	$r_\beta(12)$		ZF
14	A''	795					$\gamma_\alpha(64)$	$r_\beta(16)$	$r_\gamma(12)$		ZF
15	A'	861	903	906	w*		$\gamma_\alpha(47)$				DF
16	A''	898					$\gamma_\beta(42)$	$\gamma_\alpha(32)$	$\gamma_\gamma(15)$	$r_\beta(10)$	ZF
17	A'	930	927 m	929	931 vs	0.74	$\gamma_\alpha(37)$	$r_\gamma(31)$	$\gamma_\beta(11)$		ZF
18	A'	945	934 w				$\gamma_\alpha(32)$	$\omega_\alpha(13)$	$\rho(11)$	$\omega_{\rho\gamma}(10)$	DF
19	A''	1033	1018 w	1020	1019 m	0.83	$\gamma_\alpha(45)$	$\delta_\alpha(15)$	$r_\beta(11)$		DF
20	A''	1039	1045 w*	1045	1046 s	0.78	$\delta_\alpha(68)$	$\gamma_\alpha(23)$			GF
21	A'	1053	1063 s	1065	1066 s	0.57	$\delta_\alpha(76)$	$\gamma_\alpha(15)$			GF
22	A''	1089	1091 w	1091	1090 s	0.66	$r_\gamma(40)$	$r_\beta(24)$	$\gamma_\beta(12)$		DF
23	A'	1101	1112 m	1110	1111 vs	0.20	$\gamma_\beta(26)$	$r_\beta(19)$	$\gamma_\gamma(17)$	$\gamma_\alpha(13)$	DF
24	A'	1155	1129 vs	1131	1133 m	0.73	$\gamma_\alpha(33)$	$r_\beta(26)$	$\gamma_\beta(19)$	$r_\alpha(13)$	DF
25	A''	1163	1155 m	1157	1158 s	0.73	$\gamma_\beta(54)$	$r_\alpha(29)$	$\gamma_\gamma(13)$		ZF
26	A''	1215	1199 s	1201	1202 m	0.77	$\gamma_\gamma(53)$	$\gamma_\beta(36)$	$r_\gamma(11)$		ZF
27	A'	1268	1273 vs	1273	1274 vs	0.77	$\gamma_\beta(84)$				GF
28	A''	1281					$r_\alpha(58)$	$\gamma_\beta(28)$	$\gamma_\alpha(11)$		ZF
29	A'	1326	1335 s	1335	1336 m	0.54	$\gamma_\beta(90)$	$r_\beta(13)$			GF
30	A''	1339					$\gamma_\gamma(56)$	$\gamma_\beta(43)$			ZF
31	A''	1377	1374 vw				$\gamma_\gamma(54)$	$\gamma_\beta(30)$	$r_\gamma(20)$		ZF
32	A''	1448	1449 vs	1451	1451 vs	0.72	$\delta_\beta(81)$	$\gamma_\beta(20)$			GF
33	A'	1448					$\delta_\beta(79)$	$\gamma_\beta(19)$			GF
34	A'	1466	1465 s		1465 s*		$\delta_\gamma(78)$	$\gamma_\gamma(20)$			GF
35	A'	1709	1710 vvs	1708	1708 vs	0.30	$v(76)$	$r_\alpha(13)$	$\chi(6)$	$\gamma_\alpha(3)$	GF
36	A''	2124	2110 m	2110	2110 s	0.10	$d_\alpha(97)$				GF
37	A'	2127	2147 m	2148	2148 vs	0.06	$d_\alpha(97)$				GF
38	A''	2212	2217 m*	2218	2214 s	0.67	$d_\alpha(98)$				GF
39	A'	2219	2229 s	2228	2229 vs	0.48	$d_\alpha(97)$				GF
40	A'	2854	2858 s*				$d_\gamma(99)$				GF
41	A''	2877	2868 vs	2863	2863 vs	0.06	$d_\beta(99)$				GF
42	A'	2878					$d_\beta(99)$				GF
43	A'	2918	2909 vs*	2908	2906 s	0.26	$d_\gamma(96)$				GF
44	A''	2941	2942 vs	2945	2946 vs	0.20	$d_\beta(99)$				GF
45	A'	2945					$d_\beta(96)$				GF

ᵃ An asterisk denotes an inflection. ᵇ See footnote c in Table IVA.

putation to an "acceptable" solution (cf. p 446). If during the refinement a significant part of the potential energy is observed to be associated with an off-axis element of the $\mathfrak{F}$ matrix, it is indicative of a poorly chosen initial force field. Commonly this will be accompanied by a drift of the corresponding off-diagonal force constants to unrealistic values and a departure of $\Sigma_i E_{p(t)}$ from ~100.

A. CLASSIFICATION OF THE NORMAL MODES

If a normal mode of vibration is determined mainly by a single internal coordinate, it will generate a dominant coefficient in the potential energy distribution function and can be considered a "good" group frequency. To cast this into quantitative terms, it may be suggested that *not less than 66% of the potential energy should be associated with a single type of internal coordinate to warrant classification as a localized group frequency*. It will be seen from Table IVA that 19 of the 45 normal modes of 1 fulfill this condition; they are indicated as GF in the last column of the table.[61]

(61) In some cases there will be more than one internal coordinate of the same type. Thus, for example, it will be evident from Figure 2 that there are four $d\alpha$ internal coordinates, two associated with each of the $C\alpha$ atoms. The coefficient $E_{p(i)}$ indicates only the total fraction of the energy of the mode distributed among the four $d\alpha$ coordinates. Further breakdown can be made by analysis of the eigenvectors associated with this mode; this offers an additional degree of sophistication in the description of the group frequency which we shall not consider here. It has been discussed by Scherer for C–H deformation motions in chlorobenzenes.[62]

(62) J. R. Scherer, *Spectrochim. Acta, Part A*, 24, 747 (1968).

Table IVC

Cyclohexanone-$\beta,\beta,\beta',\beta',\gamma,\gamma'$-$d_6$ (3)

No.	Sym	ν, cm⁻¹	Ir^a ν, cm⁻¹	Raman,^{a} Hg arc	Δν, cm⁻¹ ρ	Potential energy distribution coefficients				Mode type
1	A′	115		91		$\omega_\alpha(30)$	$\tau_{\beta\gamma}(15)$	$\rho(12)$	$\chi(12)$	DF
2	A″	177		164		$\tau_{\beta\gamma}(45)$	$\omega_{\beta\gamma}(18)$	$\omega_\alpha(18)$		DF
3	A′	237		254	0.57	$\omega_{\beta\gamma}(30)$	$\tau_{\beta\gamma}(30)$	$\gamma_\beta(15)$	$\omega_\alpha(12)$	DF
4	A′	379	379 m	378 m	0.77	$\omega_{\beta\gamma}(41)$	$\gamma_\beta(27)$	$\gamma_\gamma(23)$	$\chi(10)$	ZF
5	A″	420	381 m	388 m	0.87	$\omega_{\beta\gamma}(37)$	$\omega_\alpha(26)$	$\gamma_\beta(23)$	$\gamma_\alpha(14)$	DF
6	A′	443	435 m	435 w	0.89	$\chi(25)$	$\gamma_\alpha(22)$	$\rho(14)$	$\epsilon(10)$	DF
7	A″	470	483 vs	486 m	0.78	$\epsilon(70)$				GF
8	A′	604	603 m	605 s	0.20	$\rho(38)$	$r_\beta(13)$	$\gamma_\gamma(10)$		DF
9	A″	651	653 s			$\gamma_\beta(58)$	$\gamma_\alpha(12)$			ZF
10	A′	681	693 m	695 vs	0.15	$r_\alpha(39)$	$\gamma_\beta(26)$	$r_\gamma(10)$		DF
11	A′	702	719 s	718 m	0.24	$\gamma_\beta(32)$	$\gamma_\gamma(25)$	$r_\alpha(12)$	$\gamma_\alpha(12)$	DF
12	A′	737	754 w	755 vs	0.18	$r_\gamma(42)$	$\gamma_\beta(34)$	$\gamma_\alpha(11)$		ZF
13	A″	756				$\gamma_\beta(51)$	$\gamma_\alpha(30)$	$\gamma_\gamma(29)$		ZF
14	A″	789	784 vw	784 m	0.85	$\gamma_\gamma(43)$	$r_\gamma(21)$	$r_\beta(15)$		DF
15	A″	850	844 vs	847 vw		$\gamma_\beta(61)$	$r_\beta(16)$			ZF
16	A′	875	897 m	897 vs	0.72	$\gamma_\beta(22)$	$r_\beta(16)$	$\gamma_\alpha(11)$	$\omega_\alpha(10)$	DF
17	A″	905	918 w	918 m*		$\gamma_\beta(35)$	$\gamma_\gamma(30)$			DF
18	A′	927	938 m	938 m		$\gamma_\beta(26)$	$r_\alpha(23)$	$\gamma_\alpha(11)$	$\omega_{\beta\gamma}(10)$	DF
19	A″	957	977 s	978 vs	0.76	$\gamma_\alpha(40)$	$\gamma_\gamma(22)$	$\gamma_\beta(18)$		DF
20	A′	976				$\gamma_\beta(54)$	$\gamma_\gamma(10)$			DF
21	A′	1040	1048 m*			$\gamma_\alpha(35)$	$\gamma_\beta(14)$	$\rho(10)$		DF
22	A″	1051	1052 s	1052 s	0.56	$\delta_\beta(79)$	$\gamma_\beta(19)$			GF
23	A′	1059				$\delta_\beta(74)$	$\gamma_\beta(17)$			GF
24	A′	1072	1080 s	1081 m		$\delta_\gamma(77)$	$\gamma_\gamma(15)$			GF
25	A″	1106	1100 m	1101 s		$\gamma_\gamma(41)$	$\gamma_\beta(32)$	$r_\beta(30)$		ZF
26	A′	1151	1133 s	1135 vw		$r_\beta(35)$	$\gamma_\beta(29)$	$\gamma_\alpha(28)$	$r_\gamma(12)$	DF
27	A″	1165	1173 m	1174 m	0.88	$\gamma_\alpha(53)$	$\gamma_\gamma(16)$	$r_\gamma(14)$	$r_\alpha(10)$	ZF
28	A″	1224	1211 m	1211 s	0.75	$r_\alpha(41)$	$\gamma_\alpha(22)$	$r_\gamma(17)$	$\epsilon(15)$	DF
29	A′	1229	1230 s	1231 s	0.71	$\gamma_\alpha(69)$	$\gamma_\beta(16)$	$r_\gamma(12)$		GF
30	A″	1257	1249 vs	1249 m*		$\gamma_\alpha(59)$	$r_\gamma(33)$	$\gamma_\beta(10)$		ZF
31	A′	1281	1289 vs	1291 w		$\gamma_\alpha(89)$	$r_\beta(16)$			GF
32	A″	1293				$\gamma_\alpha(57)$	$r_\alpha(43)$	$r_\beta(17)$		ZF
33	A′	1429	1424 vs	1424 vs	0.92	$\delta_\alpha(82)$	$\gamma_\alpha(19)$			GF
34	A″	1430	1432 vs			$\delta_\alpha(80)$	$\gamma_\alpha(20)$			GF
35	A′	1715	1716 vvs	1714 vs	0.49	$v(75)$	$r_\alpha(13)$	$\chi(6)$	$\gamma_\alpha(5)$	GF
36	A′	2090	2096 s*	2099 vs	0.28	$d_\gamma(96)$				GF
37	A″	2107	2110 vs	2107 s*		$d_\beta(97)$				GF
38	A′	2108	2120 vs*	2122 vs	0.31	$d_\beta(95)$				GF
39	A′	2178	2185 s	2185 s*		$d_\gamma(80)$	$d_\beta(18)$			GF
40	A″	2196	2209 vs	2209 vs	0.68	$d_\beta(98)$				GF
41	A′	2210	2220 s*	2223 s*		$d_\beta(80)$	$d_\gamma(16)$			GF
42	A″	2900	2900 vs	2899 vs	0.25	$d_\alpha(99)$				GF
43	A′	2901				$d_\alpha(99)$				GF
44	A″	2964	2965 vs	2961 vs	0.48	$d_\alpha(99)$				GF
45	A′	2966				$d_\alpha(99)$				GF

^{a} An asterisk denotes an inflection.

Fourteen of the remaining normal modes are described by two $E_{p(t)}$ coefficients that together account for about 66% of the energy. In all cases these are associated with vicinal motions involving neighboring carbon atoms, though the form of the vibration may be too complex to be readily conceptualized. These are indicated as ZF (zone frequency) in Tables IVA–IVD. A typical example is band no. 23 in **1**, calculated at 1238 cm⁻¹ and observed in the infrared spectrum at 1247 cm⁻¹. The potential energy distribution is $\gamma_\beta(52) + \gamma_\alpha(34)$, indicating that it is a coupled methylene bend motion in which both C_α and C_β atoms participate; it is one of several methylene deformation modes. Though it can be localized in the two $C_\alpha H_2$–$C_\beta H_2$ moieties it would be meaningless to cat-

egorize it more specifically in group frequency terminology as a wag or twist in-phase motion.

In a somewhat different context the term "zone pattern" has been used in the quantitative classification of steroid spectra to characterize sets of bands that can be correlated on purely empirical grounds with specific structural zones in the molecule.[5-9] In line with this terminology it is useful to designate these quasi-group frequencies as *zone frequencies;* normal coordinate analysis identifies them with localized regions of the molecule, but the motions of the atoms are too complex and the molecular structural units too large to justify their identification with group frequencies as that term is commonly used by organic chemists. These zone frequencies are sensitive

Table IVD

Cyclohexanone-d_{10} (4)

No.	Sym	Calcd ν, cm⁻¹	Ir[a] ν, cm⁻¹	Raman[a] Hg arc ν	$\Delta\nu$, cm⁻¹ ρ	Potential energy distribution coefficients	Mode type
1	A′	109		93		$\omega_\alpha(30)$ $\tau_{\beta\gamma}(14)$ $\chi(13)$ $\rho(11)$	DF
2	A″	162		163		$\tau_{\beta\gamma}(45)$ $\omega_{\beta\gamma}(21)$ $\omega_\alpha(15)$	ZF
3	A′	232		254 m	0.62	$\omega_{\beta\gamma}(32)$ $\tau_{\beta\gamma}(32)$ $\gamma_\beta(13)$ $\omega_\alpha(10)$	DF
4	A′	370	349 m	351 s		$\gamma_\alpha(26)$ $\chi(26)$ $\rho(18)$ $\epsilon(11)$	DF
5	A′	379		381 m		$\omega_{\beta\gamma}(40)$ $\gamma_\beta(34)$ $\gamma_\gamma(25)$ $\gamma_\alpha(12)$	ZF
6	A″	388	368 w	366 s	0.81	$\omega_{\beta\gamma}(27)$ $\gamma_\alpha(25)$ $\omega_\alpha(24)$ $\gamma_\beta(22)$	DF
7	A″	450	450 vs	452 s	0.70	$\epsilon(65)$	GF
8	A′	583	580 m	583 vs	0.25	$\rho(26)$ $\gamma_\alpha(12)$ $\gamma_\gamma(12)$ $r_\beta(12)$	DF
9	A″	616	612 m			$\gamma_\beta(37)$ $\gamma_\alpha(29)$	ZF
10	A′	655	655 w*			$\gamma_\alpha(32)$ $\gamma_\gamma(28)$ $\gamma_\beta(25)$	DF
11	A′	665	667 m	667 s	0.22	$r_\alpha(48)$ $\gamma_\beta(21)$	ZF
12	A″	702	682 vw			$\gamma_\beta(42)$ $\gamma_\alpha(33)$ $\gamma_\gamma(23)$	ZF
13	A′	708	721 vw	721 vs	0.16	$r_\gamma(51)$ $\gamma_\alpha(16)$ $\gamma_\beta(14)$ $r_\beta(10)$	ZF
14	A″	738	739 m	744 w		$r_\beta(25)$ $\gamma_\alpha(24)$ $\gamma_\gamma(20)$ $r_\gamma(13)$	DF
15	A′	789	787 m	788 s	0.01	$\gamma_\beta(39)$ $\gamma_\alpha(35)$ $r_\beta(11)$	ZF
16	A″	800				$\gamma_\alpha(78)$ $\gamma_\beta(16)$ $\gamma_\gamma(10)$	GF
17	A″	818	827 w			$\gamma_\beta(46)$ $\gamma_\gamma(34)$	ZF
18	A′	829	863 w			$\gamma_\alpha(33)$ $\omega_{\beta\gamma}(17)$	DF
19	A″	892	889 m	892 m	0.75	$\gamma_\beta(46)$ $\gamma_\gamma(18)$ $r_\beta(10)$	DF
20	A′	905	922 w			$\gamma_\alpha(50)$ $\gamma_\beta(12)$	DF
21	A′	954	930 w	933 s	0.72	$\gamma_\beta(50)$ $\gamma_\alpha(13)$ $\rho(11)$	DF
22	A″	971	968 m	971 m	0.78	$\gamma_\gamma(33)$ $\gamma_\alpha(22)$ $\gamma_\beta(15)$	DF
23	A″	1015	1016 s			$\gamma_\alpha(57)$ $\gamma_\beta(23)$ $\epsilon(11)$	ZF
24	A′	1015	1002 m*	1002 m	0.12	$\gamma_\beta(26)$ $\gamma_\gamma(16)$ $\gamma_\alpha(13)$	DF
25	A″	1039	1048 s*			$\delta_\alpha(79)$ $\gamma_\alpha(18)$	GF
26	A′	1048	1056 s	1054 m		$\delta_\alpha(66)$ $\gamma_\alpha(18)$	GF
27	A″	1055	1067 s	1069 s	0.89	$\delta_\beta(76)$ $\gamma_\beta(17)$	GF
28	A′	1059				$\delta_\beta(69)$ $\gamma_\beta(16)$	GF
29	A′	1074	1079 s	1080 s		$\delta_\gamma(67)$ $\gamma_\gamma(12)$	GF
30	A′	1097	1095 s	1098 s	0.19	$\gamma_\alpha(41)$ $\gamma_\beta(28)$ $r_\alpha(18)$ $r_\gamma(15)$	ZF
31	A″	1116	1116 m			$\gamma_\gamma(36)$ $r_\beta(31)$ $\gamma_\beta(25)$	ZF
32	A′	1196	1191 vs	1194 m*		$r_\beta(53)$ $\gamma_\beta(33)$ $r_\gamma(18)$ $\gamma_\alpha(12)$	ZF
33	A″	1224	1221 m			$r_\gamma(61)$ $\gamma_\gamma(21)$ $r_\alpha(16)$ $\gamma_\beta(16)$	ZF
34	A″	1258	1245 vs	1249 m		$r_\alpha(72)$ $r_\beta(22)$ $\gamma_\alpha(12)$	GF
35	A′	1709	1710 vvs	1709 vs	0.55	$v(76)$ $r_\alpha(13)$ $\chi(6)$ $\gamma_\alpha(3)$	GF
36	A′	2090	2083 m*	2086 m*		$d_\gamma(96)$	GF
37	A″	2107	2111 vs	2109 vs	0.34	$d_\beta(97)$	GF
38	A′	2108				$d_\beta(94)$	GF
39	A″	2123	2125 s*	2126 s	0.29	$d_\alpha(97)$	GF
40	A′	2126				$d_\alpha(96)$	GF
41	A′	2178	2165 m	2165 m	0.33	$d_\gamma(81)$ $d_\beta(16)$	GF
42	A″	2193	2210 vs	2213 vs	0.64	$d_\beta(83)$ $d_\alpha(16)$	GF
43	A′	2204				$d_\beta(60)$ $d_\alpha(28)$ $d_\gamma(10)$	ZF
44	A″	2215	2221 s*			$d_\alpha(83)$ $d_\alpha(15)$	GF
45	A′	2225				$d_\alpha(69)$ $d_\beta(21)$	GF

[a] An asterisk denotes an inflection.

to small changes in structure; in many cases it would be questionable to seek for the exact counterparts of such zone frequencies in the spectra of related deuterated species.
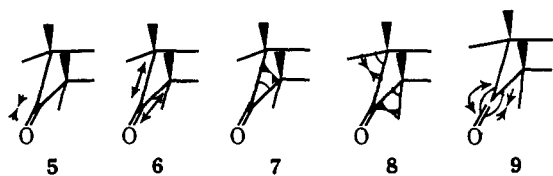
There remains a third category of normal modes in which the potential energy is spread fairly evenly over many internal coordinates. These can be designated *delocalized frequencies*. In large nonsymmetric molecules they can only be described nonspecifically as skeletal modes, ring breathing modes, etc., and are indicated as DF in Tables IVA–IVD. Where the symmetry is higher, definitive descriptions are sometimes possible. For example, the in-phase, out-of-plane C–H deformations of substituted benzenes belong in this category, yet some of these modes are included in the organic chemist's catalog of useful characteristic group frequencies.

B. VIBRATIONAL MODES INVOLVING C=O

The three internal coordinates associated with the carbonyl group are the stretch (v), the in-plane bend (ϵ), and the out-of-plane bend (ρ) (*cf.* Figure 2). *A priori*, three corresponding group frequencies might be expected. The stretch plays a major part in organic structure analysis, but the two other vibrations have only minor value for structural diagnosis. It is to be emphasized that in this context "in-plane" and "out-of-plane" relate to the local site symmetry of the C–CO–C group and not to the symmetry plane of cyclohexanone.

The "C=O stretching band" is calculated for **1** at 1715 cm⁻¹ and observed at 1718 cm⁻¹ in the infrared and at 1710 cm⁻¹ in the Raman spectrum. It is displaced to 1709 cm⁻¹

Table V

Vibrational Motions Participating in the "Carbonyl Stretch Band," Expressed as Potential Energy Coefficients ($E_{p(i)}$)

5	6	7	8	9

		5 (v)	6 (r_α)	7 (x)	8 (γ_α)^a	9 (ϵ)
No.						
1	$\nu_{calcd} = 1715$ cm^{-1}	75	13	6	5	2
2	$\nu_{calcd} = 1709$ cm^{-1}	76	13	6	3	2
3	$\nu_{calcd} = 1715$ cm^{-1}	75	13	6	5	2
4	$\nu_{calcd} = 1709$ cm^{-1}	76	13	6	3	2

Structure^b

^{a} There are four γ_α internal coordinates associated with each C_α atom, but eigenvector analysis indicates that the energy is concentrated to the extent of about 85% in the in-plane motion illustrated in **8**. ^{b} In all dynamic structural formulas expansion is indicated by $\leftrightarrow$ and contraction by $\rightarrow \leftarrow$; these correspond with + and − eigenvectors in the calculations.

(calcd) by α-deuterium substitution in **2** and **4** and is unchanged by β-deuterium substitution in **3**. The potential energy coefficients indicate that five internal coordinates participate significantly in the 1715-cm^{-1} mode (Table V). The contribution from the C=O stretch coordinate **5** is about 75% with the other contributions coming from the symmetric stretch of the α-CC bonds **6**, two symmetric angle bends **7, 8**, and the C=O in-plane deformation **9**. There are no significant contributions from bonds more remote than the α-CH$_2$ groups.

The antisymmetric C=O in-plane deformation **10** can be primarily identified with the strong infrared band at 490 cm^{-1} in **1**. It is slightly shifted to 483 cm^{-1} by β deuteration (**3**) and more sharply by α deuteration (**2** and **4**). The potential energy coefficient of the in-plane C=O bend coordinate is about 70 in **1** and **3** and falls below 66 in **2** and **4**. The remainder of the energy resides mainly in the antisymmetric α-CC bend (**11**)

10	11
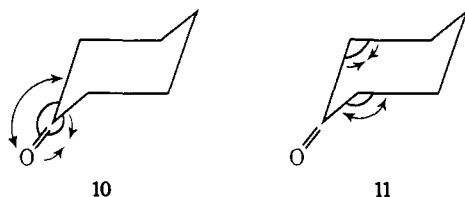
with smaller contributions from the α-CC and β-CC stretch coordinates and from β-CCC bends. This band therefore is marginally recognizable as a group frequency, but the coupling with the ring system is appreciable and can be observed out of the C$_\beta$ atoms.

The C=O out-of-plane deformation of **1** is distributed among several A′ modes and couples strongly with CC bend coordinates. The main contribution (*ca.* 30%) is to the band at 653 cm^{-1} in **1**, 615 cm^{-1} in **2**, 604 cm^{-1} in **3**, and 581 cm^{-1} in **4**. This is a highly delocalized mode and is discussed further below. It is meaningless to attempt to characterize any band in these spectra as "the C=O out-of-plane wag," but it would be hazardous to generalize that C=O out-of-plane wag vibrations are always delocalized in this manner. It is not so in

Table VI

Positions of the Skeletal Vibrations (cm^{-1} obsd)

Structure	I	II	III	IV	V	VI	VII^a	VIII^b
1	106	188	312	410	460	490	490	653
2	101	175	307	360	391	454	454	615
3	91	164	254	435	384	378	485	604
4	93	163	254	350	367	381	451	581

^{a} Identified with the C=O in-plane wag (see text). ^{b} Marginally identified with the C=O out-of-plane wag (see text).

cyclopentanone,[20] and it is stated in the literature that in some compounds this motion is considered a "good" group frequency.[63]

C. LOW-FREQUENCY SKELETAL VIBRATIONS

There are eight skeletal modes below 700 cm^{-1} of which five are symmetric (A′) and three antisymmetric (A″). These can be correlated through the isotopic series as shown in Table VI. Of these, band VII can be identified with the asymmetric C=O in-plane wag (**10**) as noted above, but the others are strongly mixed and involve CC stretch and torsions, CCC bends, and the related motions of the O=CC moiety.

The lowest frequency band I is a highly delocalized symmetric ring distortion in which all the CCC angles change and the CC torsions and the C=O out-of-plane wag also participate. No single internal coordinate contributes more than about 32% of this mode. Band II at 188 cm^{-1} in **1** is an antisymmetric out-of-plane ring distortion, mostly involving twist of the β-CC bonds and α-CCC and β-CCC angle bends. III has its main contribution from twist of the γ-CC bonds coupled with bend of the β- and γ-CCC angles. The C–CO–C angle bend 7 participates prominently in IV and is sharply sensitive to α deuteration. The symmetric mode VI at 490 cm^{-1} is superimposed on the strong antisymmetric C=O in-plane vibration discussed above; it contains a high contribution from the β-CCC angle bends and is sensitive to β deuteration.

These complex skeletal motions can be visualized by the use of flexible models in conjunction with the potential energy coefficient data from Tables IVA–IVD. In this way it can be shown, for example, that band II constitutes a partial flipping toward a chair → boat conformation inversion.[65]

D. BENDING VIBRATIONS INVOLVING METHYLENE GROUPS

In **1** there are 26 vibrational modes between 700 and 1500 cm^{-1}, all of which involve HCH and HCC angle bends. The

(63) See p 183 of ref 1. In acetone, Cossee and Schachtschneider[41] find the C=O out-of-plane wag to contribute about 86% to the band near 390 cm^{-1}. Shimizu and Shingu[64] claim that for open-chain carbonyls O=CXY (X, Y = H, CH$_3$, halogen) good correlations can be established between the frequency of the C=O out-of-plane wag and the electronegativity of the substituent; however, they assign this vibration to the band at 490 cm^{-1} in acetone, which the calculation of Cossee and Schachtschneider indicate to be predominantly the in-plane C=O deformation.

(64) K. Shimizu and H. Shingu, *Spectrochim. Acta*, 22, 1528 (1966).

(65) These motions can also be demonstrated by a computer graphic technique which will display the modes directly in terms of the eigenvectors computed from the refined normal coordinate data used directly as input to the program. Computer programs to do this are being developed but they are not yet able to deal with molecules of this complexity.

Table VII

Positions of the CH_2 and CD_2 Scissor Modes[a]

Structure		1	2	3	4
	C_γ	1466 (1463)	1466 (1465)	1072 (1080)	1074 (1079)
	oop C_β	1448 (1450)	1448 (1450)	1051 (1052)	1055 (1067)
	ip C_β	1449 (1450)	1448 (1450)	1059 (1052)	1059 (1067)
	oop C_α	1430 (1429)	1039 (1045)	1430 (1432)	1039 (1048)
	ip C_α	1429 (1422)	1053 (1064)	1429 (1424)	1048 (1055)

[a] In cm^{-1}; observed values are given in parentheses; oop = out of phase; ip = in phase.

CH_2 scissor vibrations are comparatively pure, but the others couple extensively with one another and with the skeletal CC stretches. The calculated frequencies associated with CH_2 and CD_2 scissor motions are summarized in Table VII. In all cases the potential energy coefficients of the CH_2 bend coordinates are in the range 78–80 and CD_2 bends in the range 66–82. The remaining energy comes almost wholly from CH_2 rock–twist at the same carbon atom, and there is negligible coupling with the skeletal CC stretch. These scissor vibrations therefore behave as purer group frequencies than the C=O stretch. The calculations confirm the empirically well-established displacement of the C_α methylene scissor to lower frequency; they also indicate that a small downward shift is induced at the C_β methylene, while the C_γ methylene scissor occurs at the same frequency as in the infinite *trans*-polymethylene chain.[13] It has been noted on p 448 that systematic effects paralleling these are observed in the CH bend and CC stretch force constants. At each of the two C_α and C_β atoms the scissor motions may be in-phase or out-of-phase with one another. The experimental data suggest that at C_α there is sufficient coupling through the C_α–CO–C_α system to produce a frequency difference of 7 cm^{-1} in 1 and 8 cm^{-1} in 3 between the in-phase and out-of-phase scissor modes. At C_β no difference is observed. The effect at C_α is only marginally apparent in the calculated data.

Classification of the various HCC and HCH bend vibrations below 1400 cm^{-1} in terms of rock, wag, or twist is not generally possible since the motions are too complex; for the most part they cannot even be assigned to a single carbon atom because of coupling with the CC stretch vibrations. From Tables IVA–IVD it is seen that only in a few instances does any one type of internal coordinate contribute 50% to the mode energy. The two bands calculated at 1344 and 1205 cm^{-1} in 1 approximate reasonably well to in-phase C_β-methylene wag and C_β-methylene twist, respectively. In 3 the α-CH_2

deformation modes are largely decoupled from the C motions because of the mass difference accompanying the change from CH_2 to CD_2 on the C_β atom; thus the 1281-cm^{-1} band of 3 is a fairly pure symmetric α-CH_2 wag. In the majority of the other bands, coupling between adjacent carbon atoms is such that the motions cannot be localized to units smaller than –CX_2–CX_2– (X = H, D) though in many instances only two C atoms are involved with close to 50% of the energy associated with each of the two methylene moieties.

This is the characteristic "fingerprint" region of the infrared spectrum, and it is not difficult to extrapolate to more complex alicyclic structures and gain some insight into the nature of the transferable zone patterns observed in steroid spectra.

E. CH AND CD STRETCH VIBRATIONS

The calculated frequencies occurring in the range 2000–3000 cm^{-1} are summarized in Table VIII. The potential energy coefficient data in Tables IVA–IVD show that the CH stretch vibrations are all pure group frequencies with more than 90% potential energy localization in the C–H bonds. In 1 the CH stretch frequencies associated with C_α, C_β, and C_γ differ slightly and can be correlated with bands in the observed spectra. The frequency differences calculated for the in-phase and out-of-phase modes are very small (1–3 cm^{-1}) and are not detected in the measured spectra. The α-CD_2 groups in 2 exhibit similar localization, but in 3 there are indications of couplings between the out-of-phase stretch vibrations in the $C_\beta D_2$–$C_\gamma D_2$–$C_\beta D_2$– structure. The localization remains high for the symmetric modes. In 4 the tendency for coupling to occur between the antisymmetric CD stretch motions of adjacent CD_2 groups is more evident, but the symmetric modes still remain highly localized. Coupling is strongest between the C_α and C_β atoms, but even here the energy remains localized in a dominant internal coordinate. They would still be

Table VIII

Positions of the CH_2 and CD_2 Stretch Modes[a]

Structure		1	2	3	4
	Asym C_α iph[b]	2967 (2961)	2219 (2229)[c]	2966 (2963)	2225 (2221)
	Asym C_α ooph[b]	2965 (2961)	2212 (2217)[c]	2964 (2963)	2215 (2221)
	Asym C_β iph	2944 (2949)	2945 (2944)	2210 (2220)	2204 (2210)
	Asym C_β ooph	2941 (2940)	2941 (2944)	2196 (2209)	2193 (2210)
	Asym C_γ	2918 (2920)	2918 (2909)	2178 (2185)	2178 (2165)
	Sym C_α iph	2901 (2900)	2127 (2148)[d]	2901 (2900)	2126 (2126)
	Sym C_α ooph	2900 (2894)	2124 (2110)[d]	2900 (2900)	2123 (2126)
	Sym C_β iph	2878 (2866)	2878 (2865)	2108 (2120)	2108 (2110)
	Sym C_β ooph	2877 (2866)	2877 (2865)	2107 (2110)	2107 (2110)
	Sym C_γ	2853 (2859)	2854 (2858)	2090 (2097)	2090 (2085)

[a] In cm^{-1}; ν_{calcd} is given first followed by ν_{obsd} in parentheses. Asym (antisymmetric) and Sym (symmetric) refer to the local site symmetry. [b]iph = in phase and ooph = out of phase. [c] The α-CD_2 vibrations appear split into two components and the average observed frequency of 2223 cm^{-1} is fed into the calculations. [d] See footnote c; average observed frequency 2129 cm^{-1}.

classed as marginal group frequencies by the criteria applied to the remainder of the spectra.

V. Concluding Remarks

In this paper we have examined in depth the implications to be drawn about the vibrational behavior of a moderately complex molecule by the application of normal coordinate analysis based on a selective valence force field. An assessment of the worth of such calculations to organic chemistry—as distinct from the aesthetic pleasure they generate as an intellectual exercise—can only be made when more molecules have been studied and it becomes possible to correlate the scattered work currently being done on various types of compounds.[66] Such calculations do serve to demonstrate the com-

plexity of the vibrational motions associated with the central regions of the infrared and Raman spectra (700–1300 cm^{-1}). They also explain why it is unlikely that much additional information will be gained by attempting to analyze these spectra further in terms of the group frequency hypothesis. Although the motions are complex, they can be treated in many instances as localized in well-defined structural units within the molecule and can be interpreted quasi-quantitatively, provided we adopt a model somewhat more sophisticated than the simple group frequency. With the hindsight provided by a simplified type of normal coordinate analysis, it becomes possible to look at the spectra in Figures 5 and 6 and discern

(66) This point has been well made by Califano (see pp 367–372 of ref 15).

both structural and dynamic significance in almost every peak and inflection in the curves.[67]

It would be injudicious to claim that the picture which emerges from this analysis of the potential energy coefficients is necessarily correct in all respects, but the increasing attention currently being given to normal coordinate analysis of large molecules is generating a self-consistent body of force constant data. This will make it increasingly practical for the chemical spectroscopist to recognize what are "reasonable" values for the force constants associated with specific types of bond structure. It would be no difficult matter to incorporate these range limits into the refinement program and so automate some of the "intuitive" guidance which now makes it necessary for the chemical spectroscopist to act as nursemaid when the computations begin to go astray.

For large molecules the chemist depends mainly on electron diffraction and X-ray crystallography for a physical picture of

the molecule. This picture is a static one, or, at best, outlines the thermal displacements of the atoms averaged over all vibrational modes. In the case of X-ray analysis it only describes the structure as locked into the crystal lattice. The picture which emerges from vibrational analysis breathes life into this structure. The chemical spectroscopist, however, must start with the correct static structure. In molecules with many elements of symmetry, an erroneous choice of the initial structure will become apparent from the comparisons of the infrared and Raman data, particularly from the Raman polarization. This, however, is not true for less symmetric molecules. Confusion may result unless those working in this field take care in the selection of the molecules for analysis and restrict themselves to structures for which the stable conformation is well established.

---

(67) In this article we have not considered overtone and combination bands. These will normally be weak under our experimental conditions of measurement. Above 1500 cm^{-1} weak bands attributable to combination and overtone bands occur on the wings of the C=O stretch band in the range 2700–2500 cm^{-1} and near 3420 cm^{-1} where the first overtone of the C=O stretch band is prominent. Below 1500 cm^{-1} there is an unassigned band at 980 cm^{-1} in 2 (Figure 5B) which could be a combination band. Bands not assignable to fundamentals are observed in the region 1400–1280 cm^{-1} of 4 (Figure 5D). These could be overtone-combination bands or could arise from incompletely deuterated species. More overtone structure is resolved out if the spectra are measured at low temperatures.